

Toward Large N Thermal QCD from Dual Gravity: The Heavy Quarkonium Potential

Mohammed Mia, Keshav Dasgupta, Charles Gale, Sangyong Jeon

*Ernest Rutherford Physics Building, McGill University,
3600 University Street, Montréal QC, Canada H3A 2T8*

ABSTRACT: We continue our study on the gravity duals for strongly coupled large N QCD with fundamental flavors both at zero and non-zero temperatures. The gravity dual at zero temperature captures the logarithmic runnings of the coupling constants at far IR and the almost conformal, albeit strongly coupled, behavior at the UV. The full UV completion of gauge theory is accomplished in the gravity side by attaching an AdS cap to the IR geometry described in our previous work. Attaching such an AdS cap is highly non-trivial because it amounts to finding the right interpolating geometry and sources that take us from a gravity solution with non-zero three-form fluxes to another one that has almost vanishing three-form fluxes. In this paper we give a concrete realisation of such a scenario, completing the program advocated in our earlier paper. One of the main advantage of having such a background, in addition to providing a dual description of the required gauge theory, is the absence of Landau poles and consequently the UV divergences of the Wilson loops. The potential for the heaviest fundamental quark anti-quark pairs, which are like the heavy quarkonium states in realistic QCD, can be computed and their linear behavior at large separations and zero temperature could be demonstrated. At small separations the expected Coulombic behavior appears to dominate. On the other hand, at non-zero temperatures interesting properties like heavy quarkonium type suppressions and melting are shown to emerge from our gravity dual. We provide some discussions of the melting temperature and compare our results with the Charmonium spectrum and lattice simulations. We argue that, in spite of the large N nature of our construction, certain model-independent predictions can be made.

Contents

1. Introduction	1
2. Construction of the Geometry	3
2.1 Region 1: Fluxes, Metric and the Coupling Constants Flow	11
2.2 Region 2: Interpolating Region and the Detailed Background	13
2.3 Region 3: Seven Branes, F-Theory and UV Completions	18
3. Heavy Quark Potential from Gravity	24
3.1 Computing the Nambu-Goto Action: Zero Temperature	26
3.1.1 Quark-Antiquark potential for small u_{\max}	32
3.1.2 Quark-Antiquark potential for large u_{\max}	33
3.1.3 Generic argument for confinement	35
3.2 Computing the Nambu-Goto Action: Non-Zero Temperature	37
3.2.1 Analysis of the melting temperature	40
3.3 Numerical analysis	41
4. Conclusions and Discussions	45
A. Complete analysis of a background configuration	47
B. Solution to Einstein equations	49

1. Introduction

The study of strongly interacting matter under extreme conditions of temperature and/or density is one of the most fascinating areas of contemporary subatomic physics. This program aims to explore the many facets of the *bulk* behavior of Quantum ChromoDynamics (QCD): The theory of the strong interaction. It seeks to map out the different phases allowed by QCD and the nature of the possible phase transitions connecting them or in short, to elucidate the QCD phase diagram. In this context, the existence of an exotic phase of QCD, a quark-gluon plasma, has been a prediction of lattice QCD whose details have continuously being refined over the years [1]. On the experimental front, several observables have been put forward as signature of the quark gluon plasma. These include electromagnetic radiation [2], the quenching of energetic QCD jets [3], and the dissolution (with increasing collision

centrality and energy) of heavy quark bound states according to the seminal suggestion in Ref. [4]. The Relativistic Heavy Ion Collider (RHIC), now at the end of its first decade of operation, has uncovered an intriguing set of phenomena suggestive of new physics. One of these is the observation of strong hydrodynamic flow effects, highly suggestive of a “strongly coupled” quark gluon plasma [5].

The fate of quarkonium is being analyzed at RHIC, as it was at the SPS before. A surprising fact to emerge of these studies is that the suppression of the $c\bar{c}$ ground state - the J/ψ - at RHIC is entirely comparable to that at the SPS, in spite of the much larger energy densities being reached at the first facility. This triggered many analyses with scenarios where the enhanced dissociation at RHIC was roughly compensated by an extra formation owing, for example, to quark-antiquark coalescence near hadronization [6]. Related investigations are concerned by the fate of the quarkonium spectral density above T_c , the deconfinement temperature [7]. It is fair to write that the study of quarkonium imbedded in a finite-temperature strongly interacting medium is a flourishing industry: The modifications of its spectral profile can be related to in-medium effects. A related topic of investigation on the lattice consists of calculating the quark-antiquark potential as a function of temperature [8]. These calculations show a Coulomb potential at zero temperature, with an added linear part that slowly disappears as T is raised, leading eventually to the unbinding of quarkonia bound states. Our goal in this work is to approach this softening of the potential from a different point of view.

In parallel with the studies described in the previous paragraph, the physics of hot and dense strongly interacting matter, and thus that of the quark-gluon plasma, has recently benefited from the use of a new set of techniques, germane to string theory. The gauge-string duality can indeed provide a sophisticated toolbox with which to treat strongly-coupled, strongly interacting systems [9, 10, 11]. Our purpose here is to bring closer the more traditional investigations in QCD with those pursued in string theory. In gauge-string duality, a finite-temperature medium is dual to a black hole. Even though in a large number of applications the associated field theory is conformal, we use a framework which is “QCD-like”. More specifically, we construct the dual gravity of thermal field theory which becomes almost conformal in the UV but has logarithmic running of coupling in the IR with matter in the fundamental representation. Without being explicitly QCD, this string theory will provide some of the features associated with large N Quantum Chromodynamics, and its study may shed more light on the behavior of strongly coupled, strongly interacting matter at finite temperature.

Our paper is organized as follows: In the next section we define the geometry in which our solution will exist. The description of the full geometry is subtle, so we will divide the geometry in three regions. The far IR geometry will be described in sec. 2.1, and the far UV geometry will be described in sec. 2.3. These two geometries are connected by an interpolating geometry that we will describe in details in sec.

2.2. Once we have the full geometry, we compute the heavy quark potential from the Nambu-Goto action first for zero, and then for finite temperature in sec. 3. In this section we will also provide a generic argument for confinement both for zero and non-zero temperatures. Although most of our analysis in this paper will be done analytically, we will do some detailed numerical analysis to study regimes that are difficult to access analytically. We will show that the numerical analysis fits consistently with the expected behavior of the heavy quarkonium states in this theory. Finally, we summarize and conclude.

2. Construction of the Geometry

Following the development in [12], in [13] it was shown that a geometry where the dual thermal field theory was almost conformal in the UV, and had a logarithmic running of the coupling in the IR existed. The gauge theory studied in [13] had a dual weakly coupled gravity description at zero temperature in terms of a warped deformed conifold with seven branes and fluxes. The gauge theory in turn is strongly coupled with a *smooth* RG flow but no well defined colors at any given scale. When the gauge theory is weakly coupled, the description can be presented in terms of cascades of Seiberg dualities that slows down quite a bit when one approaches the far IR because of the presence of fundamental flavors. There is no supergravity dual description available for this case, and the cascade is only captured by the full string theory on the relevant geometry.

Once a non-zero temperature is switched on, the strongly coupled gauge theory description is given by a dual supergravity solution on a *resolved* warped deformed conifold with seven branes and fluxes [13]. The resolution factor is directly related to the temperature because in the presence of a black hole a consistent solution of the system can only be achieved by introducing a non-zero resolution factor for the two cycle. In a Klebanov-Tseytlin type geometry, this resolution factor would in fact remove the naked singularity.

One of the other key ingredient of the solution presented in [13] is the far UV picture. In all the previous known attempts to this problem, the dual supergravity solution was always afflicted by the presence of Landau Poles. Such problems arose because of the behavior of the axio-dilaton, that typically blows up due to their logarithmic behavior. What we pointed out in [13] is that the logarithmic behavior, which is so ubiquitous in these constructions, appears because we are studying the theory near any one of the seven branes. In the full F-theory picture the large r behavior is perfectly finite, and in fact also has a good description in terms of the metric too. The behavior of the warp factor for large r is given by:

$$h = \sum_{\alpha} \frac{L_{(\alpha)}^4}{r_{(\alpha)}^4} \quad (2.1)$$

with $r_{(\alpha)} = r^{1+\frac{\epsilon_{(\alpha)}}{4}}$ and $\epsilon_{(\alpha)}$ is a small positive number that is a function of $g_s N_f, g_s M$ and $g_s N$ (see eq. (3.36) of [13]. The sign difference from [13] is just a matter of convention). The $\log r$ appearing in the warp factor doesn't create much of a problem at UV: the theory is perfectly holographically renormalisable, and any fluctuations of the background are under control. The fact that we can have well defined and renormalisable interactions in this background in the presence of fundamental flavors was shown, we believe for the first time, in [13] (see [14] for renormalisability argument without fundamental flavors). For the present purpose, we want to ask a slightly different question here, namely: can we construct a dual supergravity background that allows logarithmic RG flow in the IR but has a vanishing beta function at far UV? From our discussion of the UV caps in [13] it is clear what we should be looking for: we need a gravitational background that resembles OKS geometry for small r , but has a UV cap given by an asymptotic AdS geometry. To extend this configuration to high temperature, we need OKS-BH geometry¹ at small r , and asymptotic AdS-Schwarchild geometry at large r .

Such a geometry looks complicated, so we may want to ask whether we can switch off the three form fluxes and still have a dual description with running couplings. If this were possible then the analysis could be made much more simpler. It turns out however that such a simplification cannot occur in our set-up. To elucidate the last point, let us give a brief discussion.

The RG runnings of the two gauge groups in this theory are determined by the following dual maps in terms of the bulk axio-dilaton τ and NS potential B :

$$\begin{aligned} \frac{4\pi^2}{g_1^2} + \frac{4\pi^2}{g_2^2} &= \pi \operatorname{Im} \tau \\ \frac{4\pi^2}{g_1^2} - \frac{4\pi^2}{g_2^2} &= \frac{\operatorname{Im} \tau}{2\pi\alpha'} \int_{S^2} B - \pi \operatorname{Im} \tau \pmod{2\pi} \end{aligned} \quad (2.2)$$

Once we switch off B the two couplings would be the same and would induce a Shifman-Vainstein β -function of the form:

$$\frac{\partial}{\partial \log \Lambda} \frac{8\pi^2}{g_{\text{YM}}^2} = 3N - 2N(1 - \gamma_{A,B}) - N_f(1 - \gamma_q) \quad (2.3)$$

where Λ is the energy scale that is related to the radial coordinate r in the gravity side, and $\Gamma_{A,B}$ and γ_q are the anomalous dimensions of bi-fundamental and fundamental fields respectively. With such a picture of the flow, we might think that the F-theory completion might be to simply add sufficient number of seven branes parallel to the spacetime directions and wrapping the two internal two-spheres (so that they are points in the (r, ψ) plane). This simple picture would unfortunately be inconsistent

¹For more details on the construction of OKS-BH (Ouyang-Klebanov-Strassler-Black-Hole) geometry, see [13] sections 3.1 and 3.3.

with the underlying cascading dynamics as could be seen from a T-dual framework [16, 17], and therefore would be incapable of showing certain important behavior expected from this model.

To understand the problem, observe that in the T-dual picture *à la* [16], the D3-D7-conifold geometry is mapped to a configuration of D4-D6 and intersecting NS5 branes. The NS5 branes, that are T-dual to the conifold, are along x^{012345} and x^{012389} directions and have N D4 branes (T-dual of N D3 branes) between them. Everytime we cross the NS5 branes we expect extra D4 branes to appear because of the D6 branes. This is however only possible if the D6 branes are along $x^{0123457}$ which in turn would imply that in the brane side the D7 branes have to be along the radial direction. Additionally, motion of the NS5 brane would imply a B_{NS} field in the brane side that is not a constant but has at least a $\log r$ dependence along the radial direction. This means that H_{NS} is non-zero, and we need to switch on H_{RR} to satisfy the equations of motion, bringing us back to the model originally advocated in [13]!

The discussion above should convince the readers that there aren't much avenue to simplify the original proposal of [13]. The original model proposed in [13] is structurally complicated, but is possibly the *simplest* in realising some of the properties of IR large N QCD. A model simpler than this would be devoid of any interesting physics.

Once this is settled, we want to see how to construct the kind of geometry that we mentioned above. Our requirement is to impose confinement at far IR and vanishing beta function at far UV. Since the original model studied in [13] doesn't quite have the right large r behavior because the warp factor therein goes as (2.1), we need to add appropriate UV cap. However before we actually go about constructing the background, let us clarify how addition of UV caps in general can change IR geometries. One thing should of course be clear, the far IR geometries *cannot* change by the addition of UV caps. This is because the UV caps corresponding to adding non-trivial irrelevant operators in the dual gauge theory². These operators keep far IR physics completely unchanged, but physics at not-so-small energies may change a bit. So the question is how are these changes registered in our analysis? Additionally we may also want to ask how entropy of our gauge theories affected by the addition of UV caps?

Both the above questions may be answered if we could figure out how the UV caps affect the energy momentum tensors of our gauge theories. The generic form of the energy-momentum tensor that we derived in our earlier paper [13] can be

²Assuming of course that the *relevant* operators were responsible for creating the cascading dynamics from a given UV completion in the first place!

reproduced as:

$$T_{\text{medium+quark}}^{mn} = \int \frac{d^4q}{(2\pi)^4} \sum_{\alpha,\beta} \left\{ (H_{|\alpha|}^{mn} + H_{|\alpha|}^{nm}) s_{nn}^{(4)[\beta]} - 4(K_{|\alpha|}^{mn} + K_{|\alpha|}^{nm}) s_{nn}^{(4)[\beta]} \right. \\ \left. + (K_{|\alpha|}^{mn} + K_{|\alpha|}^{nm}) s_{nn}^{(5)[\beta]} + \sum_{j=0}^{\infty} \hat{b}_{n(j)}^{(\alpha)} \tilde{\mathcal{J}}^n \delta_{nm} e^{-j\mathcal{N}_{uv}} + \mathcal{O}(\mathcal{T} e^{-\mathcal{N}_{uv}}) \right\} \quad (2.4)$$

where $H_{|\alpha|}^{mn}$ and $K_{|\alpha|}^{mn}$ depend on the full background geometry via eq. (3.124) in [13] with $s_{nn}^{(p)[\beta]}$ being the Fourier coefficients. The other terms namely $\hat{b}_{n(j)}^{(\alpha)}$ and \mathcal{N}_{uv} together specify the boundary theory for a specific UV completion [13].

Now its easy to see how the UV caps would change our results. Once we add a UV cap the local region $r_c - \alpha_1 \leq r \leq r_c + \alpha_2$ near the junction³ at $r = r_c$ changes, with (α_1, α_2) being some appropriate neighborhood around r_c . This means that C_1^{mn} , A_1^{mn} and B_1^{mn} etc. in eq (3.124) of [13] would change. These changes can be registered as

$$H_{|\alpha|}^{mn} \rightarrow \tilde{H}_{|\alpha|}^{mn} \equiv H_{|\alpha|}^{mn} + (\delta C_{1(\alpha)}^{mn} - \delta A_{1(\alpha)}^{mn}) e^{-4[1-\epsilon(\alpha)]\mathcal{N}_{\text{eff}}} + \mathcal{O}(e^{-j\mathcal{N}_{uv}}) \\ K_{|\alpha|}^{mn} \rightarrow \tilde{K}_{|\alpha|}^{mn} \equiv K_{|\alpha|}^{mn} + (\delta B_{1(\alpha)}^{mn} - \delta A_{1(\alpha)}^{mn}) e^{-4[1-\epsilon(\alpha)]\mathcal{N}_{\text{eff}}} + \mathcal{O}(e^{-j\mathcal{N}_{uv}}) \quad (2.5)$$

where the last terms in both the above equations appear from additional UV degrees of freedom, $C_{1(\alpha)}^{mn}$ etc are the relevant α -th components of C_1^{mn} etc, and \mathcal{N}_{eff} is the effective number of degrees of freedom at the cutoff.

Once we know these changes, its not too difficult to figure out the changes in the entropies due to the addition of UV caps. All we need are the RHS of eq (3.220) in [13] using the results from (2.5) and taking care of the boundary temperatures T_b from the changes in the warp factors⁴. Using (2.5) the result can be written as:

$$\frac{\delta s}{s} = \left(\frac{1}{\mathcal{T}} + \frac{1}{2h(\mathcal{T})} \frac{dh(\mathcal{T})}{d\mathcal{T}} \right) \delta\mathcal{T} \quad (2.6) \\ + \frac{\int d^4q \sum_{\alpha,\beta} \left[\delta H_{|\alpha|}^{(mn)} \tilde{s}_{nn}^{(4)[\beta]} - \delta K_{|\alpha|}^{(mn)} \left(4\tilde{s}_{nn}^{(4)[\beta]} - \tilde{s}_{nn}^{(5)[\beta]} \right) \right]}{\int d^4q' \sum_{\alpha,\beta} \left[H_{|\alpha|}^{(mn)} \tilde{s}_{nn}^{(4)[\beta]} - K_{|\alpha|}^{(mn)} \left(4\tilde{s}_{nn}^{(4)[\beta]} - \tilde{s}_{nn}^{(5)[\beta]} \right) + \mathcal{O}(e^{-\mathcal{N}_{uv}}) \right]}$$

However physics that are only sensitive to far IR dynamics of our theory will not be affected by the addition of UV caps. On the other hand in all cases, far IR or not, none of our results could depend on the cut-off r_c . The results are only sensitive to the changes in IR geometries (via (2.5)) and the UV degrees of freedom (via $e^{-j\mathcal{N}_{uv}}$).

³Clearly $\alpha_1 \ll r_c$ because the far IR geometry should remain completely unaltered.

⁴There may be interesting cases where the changes in the energy-momentum tensors are compensated by the changes in the boundary temperatures. In such cases the entropies may remain unchanged. Here we will not consider such cases.

From the above discussions we see how IR geometries could be affected by the addition of UV caps. This then tells us that we cannot simply add an AdS geometry at $r = r_c$. The vanishing beta function at UV could be realised by an asymptotic AdS geometry, a geometry whose warp factor behave as r^{-4} only asymptotically. In other words we require:

$$\begin{aligned}
h &= \frac{L^4}{r^4} \left[1 + \sum_{i=1}^{\infty} \frac{a_i(\psi, \theta_j, \phi_j)}{r^i} \right] \quad \text{for large } r \\
h &= \frac{L^4}{r^4} \left[\sum_{j,k=0} \frac{b_{jk}(\psi, \theta_i, \phi_i) \log^k r}{r^j} \right] \quad \text{for small } r
\end{aligned} \tag{2.7}$$

where (θ_i, ϕ_i, ψ) are the coordinates of the internal space. Observe also that we are now identifying the small r behavior of the warp factor to the relation (2.1) given above. The precise connection will be spelled out in details below.

Let us now make this a bit more precise. We require a gauge theory with confining IR dynamics and almost free UV dynamics at zero temperature, and then we want to study this theory at a temperature higher than the deconfining temperature, as mentioned before. Our dual gravity background that could in principle reproduce the gauge theory dynamics couldn't be the pure OKS (or OKS-BH) background of [13]. We need an appropriate UV cap. Again, as we mentioned earlier, the UV cap should be asymptotically AdS. The warp factor should have the form (2.7) at UV and IR, so we need an interpolating geometry between them to have a well defined background. The logarithmic warp factor at far IR tells us that the geometry is influenced by one or a set of coincident D7 branes. These seven branes wrap the $T^{1,1}$ as in *branch 2* of [13] while extending in the radial r direction and filling up four Minkowski directions (see eq (3.9) of [13]). In particular the embedding equation for a D7 brane is given by [17, 13]

$$z \equiv r^{3/2} e^{i(\psi - \phi_1 - \phi_2)} \sin \frac{\theta_1}{2} \sin \frac{\theta_2}{2} = \mu \tag{2.8}$$

where μ is a parameter. For supersymmetric case μ would be related to the deformation parameter of the conifold. Since we don't require supersymmetry we can take μ to be arbitrary⁵. Different values of μ will tell us how far the D7 branes are from the origin $r = 0$. The N_f D7 branes may have N_f different locations given by N_f different values of μ or D7 branes may be coincident with just a single value of μ . The

⁵The issue of supersymmetry is a little subtle here. The susy can of course be broken by choosing a different μ , but can also be broken by choosing the right μ but separating the wrapped D5 branes along (θ_2, ϕ_2) directions. One may say that if we allow bound states of D5 and D7 branes we might restore zero temperature susy. Alternatively we can consider the seven-branes to be oriented as in [18] which is related to our far IR configuration. In [18] heavy fundamental quarks could still restore susy. In this paper we will not consider the seven-brane configurations of [18].

positions of the seven branes are therefore parametrised by the coordinate z . Since the seven branes are in *branch 2* of [13] their positions can be precisely parametrised by the internal coordinates (θ_2, ϕ_2) . Thus the seven branes stretch along r and can be placed at any point on the (θ_2, ϕ_2) plane⁶. Because of this distribution, as we shall see shortly, axion-dilaton field runs with the coordinate z and the running is determined by F theory.

Our UV cap, in the full F-theory picture, should allow a distribution of seven branes that could eventually reproduce the warp factors (2.7). This is however not the *only* requirement: we also want to study the potential of heavy quarkonium type bound states in our theory (this means that we need to study the bound states of very heavy quark-antiquark pairs). Which in turn implies that we require a set of seven branes as far away from the origin as possible (or, at high temperature, as far away as possible from the black hole horizon). There are a few possible ways to distribute the seven branes that might be able to reproduce the required picture. The simplest way would be to distribute the seven branes as in Figure 1 below. This

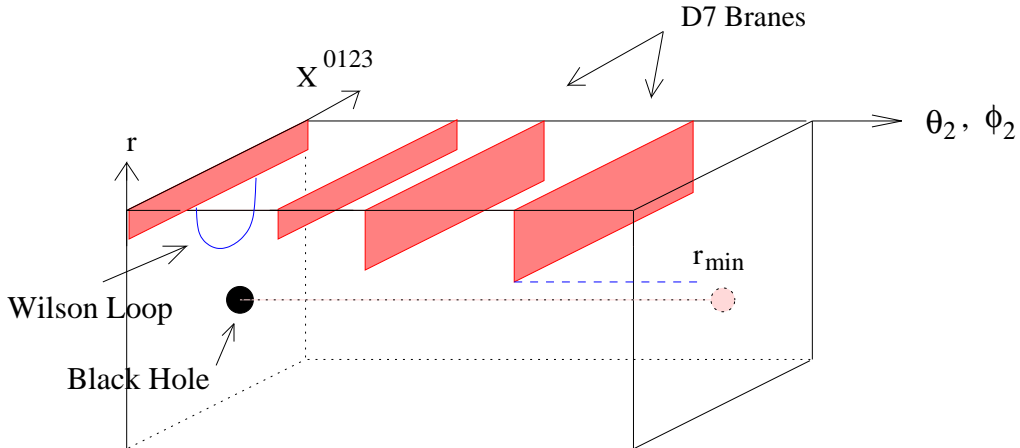


Figure 1: Simplest way to distribute localised seven branes in our model. The seven branes wrap the internal sphere parametrised by (θ_1, ϕ_1) and are stretched along the spacetime directions. Their extensions along the radial directions are parametrised by μ as in embedding equation above. The coordinate r_{\min} denote the distance of the nearest seven brane from the black hole horizon. A string stretched between this seven brane and the black hole horizon is the lightest *fundamental* quark in our model. The heaviest quark, on the other hand, will be from the seven brane that is farthest from the horizon. A string whose two ends lie on such a seven brane will form a quark antiquark bound state. The temporal evolution of such a string will determine the Wilson loop in our picture.

⁶In actual case the embedding is a union of branch 1 and branch 2. Therefore the seven-branes will trace a complicated surface in $(r, \theta_i, \phi_i, \psi)$ plane. For simplicity we will assume the embedding to be given by branch 2 of [13]. Later on when we study fluxes, the non-trivial nature of the seven-brane embeddings will become important.

picture, although simple and desirable, however does not quite suffice for us because we need a configuration of seven branes that could interpolate between the IR and UV configurations. One of the simplest way to have an interpolating geometry using the configurations studied in [13] is to make the seven branes delocalised along the (r, θ_2, ϕ_2) directions and call the resulting quantity as $\tilde{N}_f(r, \theta_2, \phi_2)$. This means that

$$N_f(r) \equiv \int d\theta_2 d\phi_2 \tilde{N}_f(r, \theta_2, \phi_2) \sin \theta_2 \quad (2.9)$$

An immediate way to realise such a configuration is given in Figure 2 below. Such a configuration has been advocated in some recent works (see for example [19, 21] where the delocalised seven branes are embedded via the Kuperstein embeddings [22]). Such

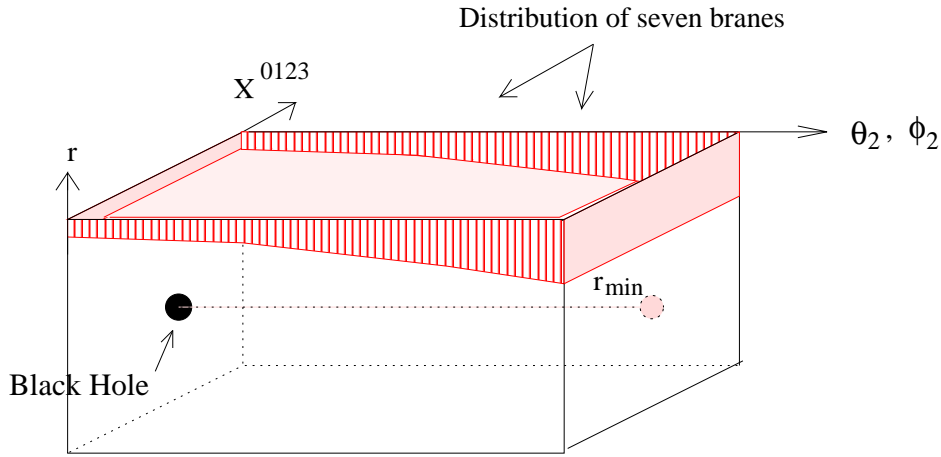


Figure 2: Complete delocalisation of the seven branes along (r, θ_2, ϕ_2) directions.

a configuration of seven branes, although useful for many purposes, unfortunately still does not quite suffice for us because heavy quarks in such a scenario would tend to go to configurations of lighter quarks spontaneously. Furthermore we want to impose the F-theory constraint, for scales $r > \hat{r}$:

$$N_f(r) \Big|_{r > \hat{r}} = 24 \quad (2.10)$$

which would be a little difficult to impose in the fully delocalised scenario⁷. Therefore the configuration that we would be mostly interested in is given in Figure 3. In this picture, which should be viewed as a cross between the earlier two figures, every individual set of seven branes are delocalised a little bit. The F-theory constraint on the number of flavors i.e (2.10) can be easily imposed without making $N_f(r, \theta_2, \phi_2)$

⁷In fact F-theory *can* allow number of seven-branes to be arbitrarily large. For this case we need to carefully study the singularity structure of the underlying manifold. Here, for most of the paper, we will restrict ourselves to 24 seven-branes. This means that g_s could be as small as 0.042.

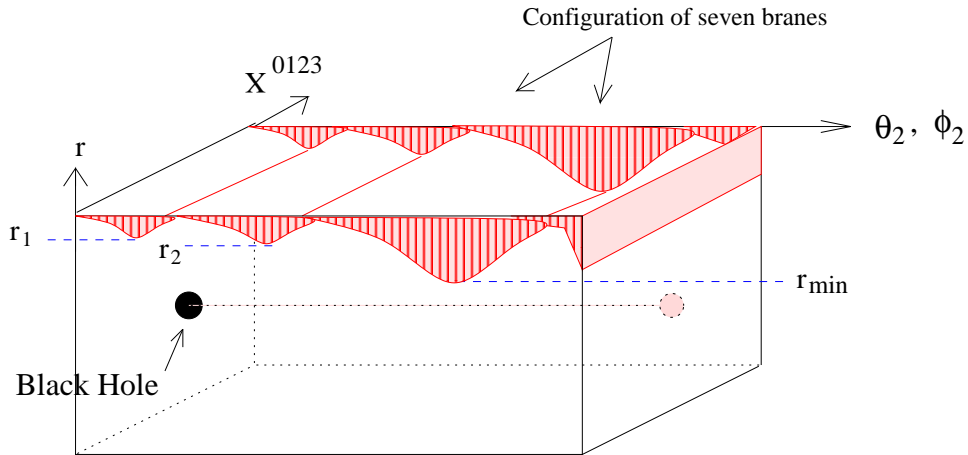


Figure 3: Another configuration of seven branes where the delocalisation is milder compared to the earlier picture. The local minima of every set of seven branes help us to study various configurations of quark antiquarks pairs.

arbitrarily small. The final picture that we want to emphasise which would capture the underlying dynamics is given as Figure 4 below. The figure is a slight variant of the previous figure. We have divided our geometry into three regions of interest: Regions 1, 2 and 3. Region 1 is basically the one discussed in great details in [13].

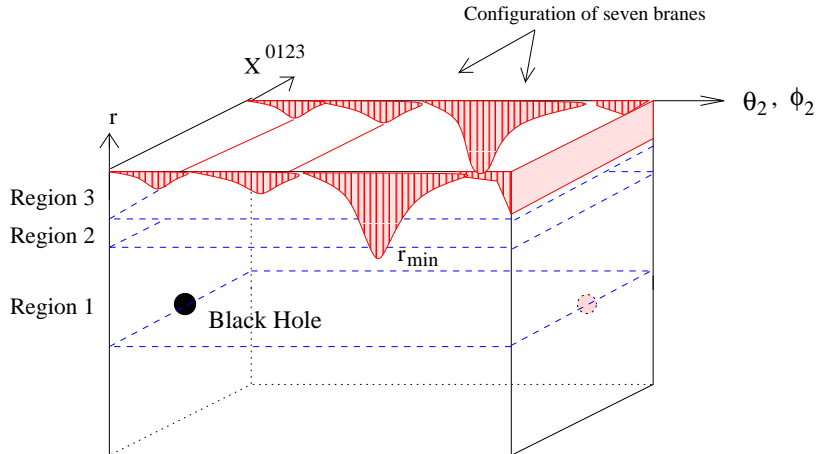


Figure 4: This figure, which is a slight variant of the previous figure, shows the various regions of interest. As should be clear, most of the seven branes lie in Region 3, except for a small number of coincident seven branes that dip till r_{\min} i.e Region 1. The interpolating region is Region 2. The detailed backgrounds for each of these regions are given in the text. Note however that, although we have emphasised Region 1 more, we will only consider the case where Region 3 \gg Region 1 + Region 2.

In this region there is one (or a coincident set of) seven brane(s). The logarithmic

dependences of the warp factor and fluxes come from these coincident (or single) seven branes. In fact the logarithmic runnings of the gauge theory coupling constants also stem from these seven branes.

Since we require UV free (or more appropriately, strongly coupled and conformal) the IR logarithmic runnings wouldn't be very desirable. Therefore the UV cap in the full F-theory framework is depicted as Region 3 in the above figure. In this region we expect all the seven branes to be distributed so that axio-dilaton has the right behavior. We also expect vanishing H_{NS} and H_{RR} fields (just like the AdS cases).

It is clear that one cannot jump from Region 1 to Region 3 abruptly. There should be an interpolating geometry where fluxes and the metric should have the necessary property of connecting the two solutions. This is Region 2 in our figure above. For all practical purposes, we expect Region 3 to dominate, in other words, Region 3 should be greater than both Regions 1 and 2 combined together. In such a scenario analysis of Wilson loop for heavy quark - antiquark bounds states would be easy: we wouldn't have to worry too much about the intermediate regions. Another big advantage about our UV cap is related to the issues raised in [23]. Since the H_{NS} and the axio-dilaton fields have well defined behaviors at large r , there would be *no* UV divergences of the Wilson loops in our picture! Therefore our configuration can not only boast of holographically renormalisability, but also of the absence of Landau poles and the associated UV divergences of the Wilson loops.

In the following, let us therefore discuss the backgrounds for all the three regions in details.

2.1 Region 1: Fluxes, Metric and the Coupling Constants Flow

The background for Region 1 is discussed in details in [13], so we will be brief. All the logarithmic behaviors for the fluxes and metric come from the single set of seven branes. The metric has the following typical form:

$$ds^2 = \frac{1}{\sqrt{h}} \left[-g_1(r)dt^2 + dx^2 + dy^2 + dz^2 \right] + \sqrt{h} \left[g_2(r)^{-1}dr^2 + d\mathcal{M}_5^2 \right] \quad (2.11)$$

where $g_i(r)$ are the black-hole factors and $d\mathcal{M}_5^2$ is the metric of warped resolved-deformed conifold (see the form in eq (3.5) of [13]). The internal space retains its resolved-deformed conifold form upto $\mathcal{O}(g_s N_f)$. Beyond this order the internal space loses its simple form and becomes a complicated non-Kähler manifold. The warp factor to this order, in terms of N_f^{eff} , M_{eff} (see eq (3.10) of [13] for details), is:

$$h = \frac{L^4}{r^4} \left[1 + \frac{3g_s M_{\text{eff}}^2}{2\pi N} \log r \left\{ 1 + \frac{3g_s N_f^{\text{eff}}}{2\pi} \left(\log r + \frac{1}{2} \right) + \frac{g_s N_f^{\text{eff}}}{4\pi} \log \left(\sin \frac{\theta_1}{2} \sin \frac{\theta_2}{2} \right) \right\} \right] \quad (2.12)$$

As discussed in [13], the background has *all* the type IIB fluxes switched on, namely, the three-forms, five-form and the axio-dilaton. Both N_f^{eff} and M_{eff} are different from

N_f and M . We will give detailed reason for this when we discuss the full geometry in the next two subsections. The three-form fluxes are:

$$\begin{aligned}
\tilde{F}_3 &= 2M_{\text{eff}}\mathbf{A}_1 \left(1 + \frac{3g_s N_f^{\text{eff}}}{2\pi} \log r \right) e_\psi \wedge \frac{1}{2} (\sin \theta_1 d\theta_1 \wedge d\phi_1 - \mathbf{B}_1 \sin \theta_2 d\theta_2 \wedge d\phi_2) \\
&\quad - \frac{3g_s M_{\text{eff}} N_f^{\text{eff}}}{4\pi} \mathbf{A}_2 \frac{dr}{r} \wedge e_\psi \wedge \left(\cot \frac{\theta_2}{2} \sin \theta_2 d\phi_2 - \mathbf{B}_2 \cot \frac{\theta_1}{2} \sin \theta_1 d\phi_1 \right) \\
&\quad - \frac{3g_s M_{\text{eff}} N_f^{\text{eff}}}{8\pi} \mathbf{A}_3 \sin \theta_1 \sin \theta_2 \left(\cot \frac{\theta_2}{2} d\theta_1 + \mathbf{B}_3 \cot \frac{\theta_1}{2} d\theta_2 \right) \wedge d\phi_1 \wedge d\phi_2 \quad (2.13) \\
H_3 &= 6g_s \mathbf{A}_4 M_{\text{eff}} \left(1 + \frac{9g_s N_f^{\text{eff}}}{4\pi} \log r + \frac{g_s N_f^{\text{eff}}}{2\pi} \log \sin \frac{\theta_1}{2} \sin \frac{\theta_2}{2} \right) \frac{dr}{r} \\
&\quad \wedge \frac{1}{2} \left(\sin \theta_1 d\theta_1 \wedge d\phi_1 - \mathbf{B}_4 \sin \theta_2 d\theta_2 \wedge d\phi_2 \right) + \frac{3g_s^2 M_{\text{eff}} N_f^{\text{eff}}}{8\pi} \mathbf{A}_5 \left(\frac{dr}{r} \wedge e_\psi - \frac{1}{2} de_\psi \right) \\
&\quad \wedge \left(\cot \frac{\theta_2}{2} d\theta_2 - \mathbf{B}_5 \cot \frac{\theta_1}{2} d\theta_1 \right)
\end{aligned}$$

where $\tilde{F}_3 \equiv F_3 - C_0 H_3$, C_0 being the ten dimensional axion and the so-called asymmetry factors $\mathbf{A}_i, \mathbf{B}_i$ are given in eq. (3.83) of [13] (see also [15]). The axio-dilaton and the five-form fluxes are:

$$\begin{aligned}
C_0 &= \frac{N_f^{\text{eff}}}{4\pi} (\psi - \phi_1 - \phi_2) \\
e^{-\Phi} &= \frac{1}{g_s} - \frac{N_f^{\text{eff}}}{8\pi} \log (r^6 + 9a^2 r^4) - \frac{N_f^{\text{eff}}}{2\pi} \log \left(\sin \frac{\theta_1}{2} \sin \frac{\theta_2}{2} \right) \\
F_5 &= \frac{1}{g_s} [d^4 x \wedge dh^{-1} + *(d^4 x \wedge dh^{-1})] \quad (2.14)
\end{aligned}$$

with a being the resolution parameter of the internal space that depends on the horizon radius r_h as $a = a(r_h) + \mathcal{O}(g_s^2 M_{\text{eff}} N_f^{\text{eff}})$. Once we consider the slice:

$$\theta_1 = \theta_2 = \pi, \quad \phi_i = 0, \quad \psi = 0 \quad (2.15)$$

the background along the slice simplifies quite a bit. To $\mathcal{O}(g_s N_f)$ the background is:

$$\begin{aligned}
h &= \frac{L^4}{r^4} \left[1 + \frac{3g_s M_{\text{eff}}^2}{2\pi N_{\text{eff}}} \log r \left\{ 1 + \frac{3g_s N_f^{\text{eff}}}{2\pi} \left(\log r + \frac{1}{2} \right) \right\} \right] \\
H_3 &= \tilde{F}_3 = C_0 = 0 \\
e^{-\Phi} &= \frac{1}{g_s} - \frac{N_f^{\text{eff}}}{8\pi} \log (r^6 + 9a^2 r^4) \quad (2.16)
\end{aligned}$$

alongwith F_5 given by (2.14). The simplicity of the background is the reason why our analysis of the mass and the drag of the quark in [13] were straightforward enough

to see the underlying physics, yet were not afflicted by problems like UV divergences of [23]⁸. Note that the logarithmic RG flows of the two couplings come from the logarithmic B_{NS} field, leading to confinement at the far IR (at zero temperature). In the following, to avoid clutter, (N, N_f, M) would denote their effective values.

2.2 Region 2: Interpolating Region and the Detailed Background

To attach a UV cap that allows a vanishing beta function we need at least a configuration of vanishing NS three-form. This cannot be *abruptly* attached to Region 1: we need an interpolating region. This region, which we will call Region 2, should have the behavior that at the outermost boundary the three-forms vanish, while solving the equations of motion. The innermost boundary of Region 2 – that also forms the outermost boundary of Region 1 – will be determined by the scale associated with the mass of the lightest quark, m_0 , in our system. In terms of Figure 4, this is given by region in the local neighborhood of $r_{\min} \equiv m_0 T_0^{-1} + r_h$, where T_0 and r_h are the string tension and the horizon radius respectively. We have already discussed some aspects of this in our previous paper [13] when we discussed the issue of UV caps. It is now time to spell this in more details.

The structure of the warp factor should be clear from [13]. We expect the form to look like (2.1) discussed earlier. For our purpose, it would make more sense to rewrite this in such a way that the radial r dependence shows up explicitly. For this we need to first define two functions $f(r)$ and $M(r)$ as (see Figure 5):

$$f(r) \equiv \frac{e^{\alpha(r-r_0)}}{1 + e^{\alpha(r-r_0)}}, \quad M(r) \equiv M[1 - f(r)], \quad \alpha \gg 1 \quad (2.17)$$

where the scale r_0 will be explained below and M is as before related to the effective number of five-branes (or the RR three-form charge). Note that for $r \ll r_0$, $f(r) \approx e^{r-r_0}$, whereas for $r > r_0$, $f(r) \approx 1$. Thus for r smaller than the scale r_0 , $f(r)$ is a very small quantity; whereas for r bigger than the scale r_0 , $f(r)$ is identity. In terms of $M(r)$ this means that for $r < r_0$, $M(r) \approx M$ whereas for $r > r_0$, $M(r) \rightarrow 0$. This will be useful below.

Using these functions, we see that the simplest way in which logarithmic behavior along the radial direction may go to inverse r behavior, is when the warp factor has the following form:

$$h = \frac{c_0 + c_1 f(r) + c_2 f^2(r)}{r^4} \sum_{\alpha} \frac{L_{\alpha}}{r^{\epsilon(\alpha)}} \quad (2.18)$$

where c_i are constant numbers, and the denominator can be mapped to $r_{(\alpha)}$ defined in (2.1) with $\epsilon_{(\alpha)}$ functions of $g_s N_f$, M , N and the resolution parameter a . L_{α} 's are

⁸On the slice (2.15) the pull-backs of the B -fields are zero. This means that Wilson loops or other equivalent constructions could be carried out without any interference from the logarithmic B -fields.

functions of the angular coordinates (θ_i, ϕ_i, ψ) . For other details see [13]. The warp factor h has the required logarithmic behavior as long as the exponents of r are small and fractional, and indeed switches to the inverse r behavior as soon as the exponents become integers. In [13] we gave some examples where the exponents are small and fractional numbers, and alluded to the case where they become integers⁹. Since N_f is a delocalised function, this behavior could be naturally realised now and would eventually give way to the required inverse r behavior of the warp factor in Region 3. Its at least clear that such a behavior of the warp factor do solve the background supergravity equations of motion near $r = r_{\min}$ (see [13] for a concrete example, and we will give more details on this below), however what we want to know whether such a behavior of the warp factor is generically a solution to EOM, or we need to add sources to the theory. It will turn out that we need to add sources at the outermost boundary of region 2. Question now is to figure out consistently the specific point in the radial direction beyond which Region 3 would start. This way we will know exactly *where* to add the sources and the AdS cap.

The demarcation point can be found easily by looking at the behavior of H_{NS} and H_{RR} . For this we need to use the functions (2.17) to write the RR three-form. Our ansatz for \tilde{F}_3 then is:

$$\begin{aligned} \tilde{F}_3 = & \left(a_o - \frac{3}{2\pi r g_s N_f} \right) \sum_{\alpha} \frac{2M(r)c_{\alpha}}{r^{\epsilon(\alpha)}} \left(\sin \theta_1 d\theta_1 \wedge d\phi_1 - \sum_{\alpha} \frac{f_{\alpha}}{r^{\epsilon(\alpha)}} \sin \theta_2 d\theta_2 \wedge d\phi_2 \right) \\ & \wedge \frac{e_{\psi}}{2} - \sum_{\alpha} \frac{3g_s M(r) N_f d_{\alpha}}{4\pi r^{\epsilon(\alpha)}} dr \wedge e_{\psi} \wedge \left(\cot \frac{\theta_2}{2} \sin \theta_2 d\phi_2 - \sum_{\alpha} \frac{g_{\alpha}}{r^{\epsilon(\alpha)}} \cot \frac{\theta_1}{2} \sin \theta_1 d\phi_1 \right) \\ & - \sum_{\alpha} \frac{3g_s M(r) N_f e_{\alpha}}{8\pi r^{\epsilon(\alpha)}} \sin \theta_1 \sin \theta_2 \left(\cot \frac{\theta_2}{2} d\theta_1 + \sum_{\alpha} \frac{h_{\alpha}}{r^{\epsilon(\alpha)}} \cot \frac{\theta_1}{2} d\theta_2 \right) \wedge d\phi_1 \wedge d\phi_2 \quad (2.19) \end{aligned}$$

where $a_o = 1 + \frac{3}{2\pi}$ and $(c_{\alpha}, \dots, h_{\alpha})$ are constants. One may also notice three things: first, how the internal forms get deformed near the innermost boundary of the region, second, how the function $f(r)$ appears for all the components, and finally, how N_f is, as before, not a constant but a delocalised function¹⁰. The function $f(r)$ becomes identity for $r > r_0$ and therefore $\tilde{F}_3 \rightarrow 0$ for $r > r_0$. For $r < r_0$, the corrections coming from $f(r)$ is exponentially small. Integrating \tilde{F}_3 over the topologically non-trivial three-cycle:

$$\frac{1}{2} e_{\psi} \wedge \left(\sin \theta_1 d\theta_1 \wedge d\phi_1 - \sum_{\alpha} \frac{f_{\alpha}}{r^{\epsilon(\alpha)}} \sin \theta_2 d\theta_2 \wedge d\phi_2 \right) \quad (2.20)$$

we find that the number of units of RR flux vary in the following way with respect

⁹See the section on holographic renormalisability in [13].

¹⁰We will soon see that N_f in fact is the effective number of seven-branes.

to the radial coordinate r :

$$M_{\text{tot}}(r) = M(r) \left(1 + \frac{3}{2\pi} - \frac{3}{2\pi r^{g_s N_f}} \right) \sum_{\alpha} \frac{c_{\alpha}}{r^{\epsilon(\alpha)}} \quad (2.21)$$

which is perfectly consistent with the RG flow, because for $r < r_0$, and $r \rightarrow r e^{-\frac{2\pi}{3g_s M}}$, M_{tot} decreases precisely as $M - N_f$ as the correction factor e^{r-r_0} coming from $f(r)$ is negligible. For $r > r_0$, M_{tot} shuts off completely. This also means that below r_0 , the total colors N decrease by M_{tot} exactly as one would have expected for the RG flow with N_f flavors. Using similar deformed internal forms, one can also write down the

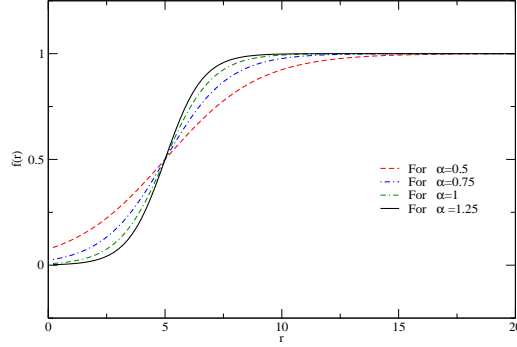


Figure 5: A plot of the $f(r)$ function for $r_0 = 5$ in appropriate units, and various choices of α . Observe that for large α the function quickly approaches 1 for $r > r_0$.

ansatze for the NS three-form. This is given as:

$$\begin{aligned} H_3 = & \sum_{\alpha} \frac{6g_s M(r) k_{\alpha}}{r^{\epsilon(\alpha)}} \left[1 + \frac{1}{2\pi} - \frac{(\text{cosec } \frac{\theta_1}{2} \text{ cosec } \frac{\theta_2}{2})^{g_s N_f}}{2\pi r^{\frac{9g_s N_f}{2}}} \right] dr \\ & \wedge \frac{1}{2} \left(\sin \theta_1 d\theta_1 \wedge d\phi_1 - \sum_{\alpha} \frac{p_{\alpha}}{r^{\epsilon(\alpha)}} \sin \theta_2 d\theta_2 \wedge d\phi_2 \right) + \sum_{\alpha} \frac{3g_s^2 M(r) N_f l_{\alpha}}{8\pi r^{\epsilon(\alpha)}} \left(\frac{dr}{r} \wedge e_{\psi} - \frac{1}{2} de_{\psi} \right) \\ & \wedge \left(\cot \frac{\theta_2}{2} d\theta_2 - \sum_{\alpha} \frac{q_{\alpha}}{r^{\epsilon(\alpha)}} \cot \frac{\theta_1}{2} d\theta_1 \right) + g_s \frac{dM(r)}{dr} \left(b_1(r) \cot \frac{\theta_1}{2} d\theta_1 + b_2(r) \cot \frac{\theta_2}{2} d\theta_2 \right) \\ & \wedge e_{\psi} \wedge dr + \frac{3g_s}{4\pi} \frac{dM(r)}{dr} \left[\left(1 + g_s N_f - \frac{1}{r^{2g_s N_f}} + \frac{9a^2 g_s N_f}{r^2} \right) \log \left(\sin \frac{\theta_1}{2} \sin \frac{\theta_2}{2} \right) + b_3(r) \right] \\ & \sin \theta_1 d\theta_1 \wedge d\phi_1 \wedge dr - \frac{g_s}{12\pi} \frac{dM(r)}{dr} \left(2 - \frac{36a^2 g_s N_f}{r^2} + 9g_s N_f - \frac{1}{r^{16g_s N_f}} - \frac{1}{r^{2g_s N_f}} + \frac{9a^2 g_s N_f}{r^2} \right) \\ & \sin \theta_2 d\theta_2 \wedge d\phi_2 \wedge dr - \frac{g_s b_4(r)}{12\pi} \frac{dM(r)}{dr} \sin \theta_2 d\theta_2 \wedge d\phi_2 \wedge dr \end{aligned} \quad (2.22)$$

with $(k_\alpha, \dots, q_\alpha)$ being constants and $b_n = \sum_m \frac{a_{nm}}{r^{m+\epsilon_m}}$ where $a_{nm} \equiv a_{nm}(a^2, g_s N_f)$ and $\tilde{\epsilon}_m \equiv \tilde{\epsilon}_m(g_s N_f)$. The way we constructed the three-forms imply that H_3 is closed. In fact the $\mathcal{O}(\partial f)$ terms that we added to (2.22) ensures that. However F_3 is not closed. We can use the non-closure of F_3 to analyse *sources* that we need to add for consistency. These sources should in general be (p, q) five-branes, with (p, q) negative, so that they could influence both the three-forms and since the ISD property of the three-forms is satisfied near $r = r_{\min}$ the sources should be close to the other boundary. A simplest choice could probably just be anti five-branes because adding anti D5-branes would change \tilde{F}_3 , and to preserve the ISD condition, H_3 would have to change accordingly. Furthermore, as we mentioned before, as $r \rightarrow r_0$, both $H_3 = \tilde{F}_3 \rightarrow 0$. Therefore $r = r_0$ is where Region 2 ends and Region 3 begins, and we can put the sources there. They could be oriented along the spacetime directions, located around the local neighborhood of $r = r_0$ and wrap the internal two-sphere (θ_1, ϕ_1) so that they are parallel to the seven-branes. However, putting in anti D5-branes near $r = r_0$ would imply non-trivial forces between the five-branes and seven-branes as well as five-branes themselves. Therefore if we keep, in general the (p, q) the five-branes close to say one of the seven-brane then they could get *dissolved* in the seven-brane as electric and magnetic gauge fluxes $*F^{(1)}$ and $F^{(1)}$ respectively. Thus the seven-brane soaks in the five-brane charges, which in turn would mean that \tilde{F}_3 in (2.19) and H_3 in (2.22) will satisfy the following EOMs:

$$\begin{aligned} d\tilde{F}_3 &= F^{(1)} \wedge \Delta_2(z) - d(\mathbf{Re} \tau) \wedge H_3 \\ d * H_3 &= * F^{(1)} \wedge \Delta_2(z) - d(C_4 \wedge F_3) \end{aligned} \quad (2.23)$$

where the tension of the seven-brane is absorbed in $\Delta_2(z)$, which is the term that measures the delocalisation of the seven branes (for localised seven branes this would be copies of the two-dimensional delta functions) and τ is the axio-dilaton that we will determine below. In addition to that $d * F_3$ will satisfy its usual EOM. For all the analysis in this paper we will also assume:

$$|r_0 - r_{\min}| \leq a_1, \quad |r_{\min} - r_h| \leq a_2, \quad \text{Region 3} \gg a_1 + a_2 \quad (2.24)$$

to be our approximation. This way, as we said before, Region 3 will dominate our calculations.

However the above set of equations (2.23) is still not the full story. Due to the anti GSO projections between anti-D5 and D7-brane, there should be tachyon between them. It turns out that the tachyon can be removed (or made massless) by switching on additional electric and magnetic fluxes on D7 along, say, (r, ψ) directions! This would at least kill the instability due to the tachyon, although susy may not be restored. For details on the precise mechanism, the readers may refer to [26]. But switching on gauge fluxes on D7 would generate extra D5 charges and switching on gauge fluxes on anti-D5s will generate extra D3 charges. This is one reason why we

write (N, N_f, M) as effective charges. This way a stable system of anti-D5s and D7 could be constructed.

To complete the rest of the story we need the axio-dilaton τ and the five-form. The five-form is easy to determine from the warp factor h (2.18) using (2.14). The total five-form charge should have contribution from the gauge fluxes also, which in turn would effect the warp factor. For regions close to r_{\min} it is clear that τ goes as $z^{-g_s N_f}$ where z is the embedding (2.8). More generically and for the whole of Region 2, looking at the warp factor and the three-form fluxes, we expect the axio-dilaton to go as¹¹:

$$\tau = [b_0 + b_1 f(r)] \sum_{\alpha} \frac{C_{\alpha}}{r^{\epsilon(\alpha)}} \quad (2.25)$$

where b_i are constants and C_{α} are functions of the internal coordinates and are complex. These C_{α} and the constants b_i are determined from the dilaton equation of motion [24, 25]:

$$\tilde{\nabla}^2 \tau = \frac{\tilde{\nabla} \tau \cdot \tilde{\nabla} \tau}{i \text{Im } \tau} - \frac{4\kappa_{10}^2 (\text{Im } \tau)^2 \delta S_{D7}}{\sqrt{-g} \delta \bar{\tau}} + (p, q) \text{ sources} \quad (2.26)$$

where tilde denote the unwarped internal metric g_{mn} , and S_{D7} is the action for the *delocalised* seven branes. The $f(r)$ term in the axio-dilaton come from the (p, q) sources that are absorbed as gauge fluxes on the seven-branes¹². Because of this behavior of axio-dilaton we don't expect the unwarped metric to remain Ricci-flat to the lowest order in $g_s N_f$. The Ricci tensor becomes:

$$\tilde{\mathcal{R}}_{mn} = \kappa_{10}^2 \frac{\partial_{(m} \partial_{n)} \tau}{4(\text{Im } \tau)^2} + \kappa_{10}^2 \left(\tilde{T}_{mn}^{D7} - \frac{1}{8} \tilde{g}_{mn} \tilde{T}^{D7} \right) + \kappa_{10}^2 \left(\tilde{T}_{mn}^{(p,q)5\text{-brane}} - \frac{1}{4} \tilde{g}_{mn} \tilde{T}^{(p,q)5\text{-brane}} \right) \quad (2.27)$$

where we see that $\tilde{\mathcal{R}}_{rr}$ picks up terms proportional to $\epsilon_{(\alpha)}^2$ and derivatives of $f(r)$, $N_f(r)$, implying that to zeroth order in $g_s N_f$ the interpolating region may not remain Ricci-flat. However since the coefficients are small, the deviation from Ricci-flatness is consequently small. In this paper we will not give the explicit form for C_{α}, L_{α} etc but it should be clear from our above discussions that EOMs are easily satisfied. The

¹¹One may use this value of axio-dilaton and the three-form NS fluxes (2.22) to determine the beta function from the relations (2.2). To lowest order in $g_s N_f$ we will reproduce the SV beta function (2.3) as expected. Notice that for $r > r_0$ the beta function *does not* vanish and both the gauge groups flow at the same rate. This will be crucial for our discussion in the following subsection.

¹²The $r^{-\epsilon(\alpha)}$ behavior stems from additional anti seven-branes that we need to add to the existing system to allow for the required UV behavior from the F-theory completion. The full picture will become clearer in the next sub-section when we analyse the system in Region 3.

one last thing to check would be the equation for the warp factor. This is given by the five-form equation of motion:

$$d * dh^{-1} = H_3 \wedge \tilde{F}_3 + \kappa_{10}^2 \text{tr} (F^{(1)} \wedge F^{(1)} - \mathcal{R} \wedge \mathcal{R}) \Delta_2(z) + \kappa_{10}^2 \text{tr} F^{(2)} \tilde{\Delta}_4(\mathcal{S}) \quad (2.28)$$

where $F^{(1)}$ is the seven-brane gauge fields that we discussed earlier, $F^{(2)}$ is the (p, q) five-brane gauge fields required for the proper interpretation of the colors in the gauge theory side¹³, \mathcal{R} is the pull-back of the Riemann two-form, and $\tilde{\Delta}_4(\mathcal{S})$ is the term that measures the delocalisation of the dissolved (p, q) five-branes over the space \mathcal{S} embedded in the seven-brane (again for localised five-branes there would be copies of four-dimensional delta functions). The $H_3 \wedge \tilde{F}_3$ term in (2.28) is proportional to $\frac{M^2(r)}{r^{2\epsilon(\alpha)}}$. This is precisely the form for the warp factor ansatz (2.18) with the $f^2(r)$ term there accounting for the $M^2(r)$ term above. This way with the warp factor (2.18) and the three-forms (2.19) and (2.22) we can satisfy (2.28) by switching on small gauge fluxes on the seven-branes and five-branes.

Therefore combining (2.18), (2.19), (2.22), (2.25) and the five-form, we can pretty much determine the supergravity background for the interpolating region $r_{\min} < r \leq r_0$. At the outermost boundary of Region 2 we therefore only have the metric and the axio-dilaton. Both the three-forms exponentially decay away fast, giving us a way to attach an AdS cap there.

2.3 Region 3: Seven Branes, F-Theory and UV Completions

The interpolating region, Region 2, that we derived above can be interpreted alternatively as the *deformation* of the neighboring geometry once we attach an AdS cap to the OKS-BH geometry. The OKS-BH geometry is the range $r_h \leq r \leq r_{\min}$ and the AdS cap is the range $r > r_0$. The geometry in the range $r_{\min} \leq r \leq r_0$ is the deformation. Such deformations should be expected for all other UV caps advocated in [13]. In this section we will complete the rest of the picture by elucidating the background from $r > r_0$ in the AdS cap. But before that let us give a brief gauge theory interpretation of background¹⁴.

For the UV region $r > r_0$ we expect the dual gauge theory to be $SU(N + M) \times SU(N + M)$ with fundamental flavors coming from the seven-branes. This is because addition of (p, q) branes at the junction, or more appropriately anti five-branes at the junction with gauge fluxes on its world-volume, tell us that the number of three-branes degrees of freedom are $N + M$, with the M factor coming from five-branes

¹³In fact one should view the gauge fluxes on the seven-branes and the five-branes as the total gauge fluxes that are needed to stabilise the system. We will see in the next subsection that the full stabilisation would require additional fluxes, but the structure would remain the same.

¹⁴The discussion in the following paragraph is motivated by a correspondence that we had with Peter Ouyang. We thank him for his comments.

anti-five-branes pairs. Furthermore, the $SU(N + M) \times SU(N + M)$ gauge theory will tell us that the gravity dual is approximately AdS, but has RG flows because of the fundamental flavors (This RG flow is the remnant of the flow that we saw in the previous subsection. We will determine this in more details below). At the scale $r = r_0$ we expect one of the gauge group to be Higgsed, so that we are left with $SU(N + M) \times SU(N)$. Now both the gauge fields flow at different rates and give rise to the cascade that is slowed down by the N_f flavors. In the end, at far IR, we expect confinement at zero temperature.

The few tests that we did above, namely, (a) the flow of N and M colors, (b) the RG flows, (c) the decay of the three-forms, and (d) the behavior of the dual gravity background, all point to the gauge theory interpretation that we gave above. What we haven't been able to demonstrate is the precise Higgsing that takes us to the cascading picture. From the gravity side its clear how this could be interpreted. From the gauge theory side it would be interesting to demonstrate this.

Coming back to the analysis of Region 3, we see that in the region $r > r_0$ we do not expect three-forms but we do expect non-zero axio-dilaton. These non-zero axio-dilaton come from the rest of the seven branes. As mentioned in [13] the complete set of seven-branes should be determined from the F-theory picture [27] to capture the full non-perturbative corrections. This is now subtle because the seven-branes are embedded non-trivially here (see (2.8)). A two-dimensional base, parametrised by a complex coordinate z , on which we can have a torus fibration:

$$y^2 = x^3 + xF(z) + G(z) \tag{2.29}$$

can be identified with the z coordinate of (2.8). This way vanishing discriminant Δ of (2.29) i.e $\Delta \equiv 4F^3 + 27G^2 = 0$, will specify the positions of the seven-branes exactly as (2.8). Here we have taken $F(z)$ as a degree eight polynomial in z and $G(z)$ as a degree 12 polynomial in z . The delocalisation $\tilde{N}_f(r, \theta_2, \phi_2)$ should be thought of somewhat as the distribution of bunches of seven branes along (θ_2, ϕ_2) directions with varying *sizes* along the radial r direction such that (2.10) is maintained with the deviation $\delta \equiv \hat{r} - r_0$ a finite but not very large number.

As is well known, embedding of seven-branes in F-theory also tells us that we can have $SL(2, \mathbf{Z})$ jumps of the axio-dilaton. We can define the axio-dilaton $\tau \equiv C_0 + ie^{-\phi}$ as the modular parameter of a torus \mathbf{T}^2 fibered over the base parametrised by the coordinate z . The holomorphic map¹⁵ from the fundamental domain of the torus to the complex plane is given by the famous j -function:

$$j(\tau) \equiv \frac{[\Theta_1^8(\tau) + \Theta_2^8(\tau) + \Theta_3^8(\tau)]^3}{\eta^{24}(\tau)} = \frac{4(24F(z))^3}{27G^2(z) + 4F^3(z)} \tag{2.30}$$

¹⁵Holomorphic in τ , the modular parameter.

where $\Theta_i, i = 1, 2, 3$ are the well known Jacobi Theta-functions and η is the Dedekind η -function:

$$\eta(\tau) = q^{\frac{1}{24}} \prod_n (1 - q^n), \quad q = e^{2\pi i \tau} \quad (2.31)$$

For our purpose, we can write the discriminant $\Delta(z)$ and the polynomial $F(z)$ generically as:

$$\Delta(z) = 4F^3 + 27G^2 = a \prod_{j=1}^{24} (z - \tilde{z}_j), \quad F(z) = b \prod_{i=1}^8 (z - z_i) \quad (2.32)$$

so that when we have weak type IIB coupling i.e $\tau = C_0 + i\infty$, $j(\tau) \approx e^{-2\pi i \tau}$ and using (2.30) the modular parameter can be mapped to the embedding coordinate z as:

$$\begin{aligned} \tau &= \frac{i}{g_s} + \frac{i}{2\pi} \log(55926ab^{-1}) - \frac{i}{2\pi} \sum_{n=1}^{\infty} \left[\frac{1}{nz^n} \left(\sum_{i=1}^8 3z_i^n - \sum_{j=1}^{24} \tilde{z}_j^n \right) \right] \\ &= \sum_{n=0}^{\infty} \frac{\mathcal{C}_n + i\mathcal{D}_n}{\tilde{r}^n} \end{aligned} \quad (2.33)$$

where $\mathcal{C}_n \equiv \mathcal{C}_n(\theta_i, \phi_i, \psi)$ and $\mathcal{D}_n \equiv \mathcal{D}_n(\theta_i, \phi_i, \psi)$ are real functions and $\tilde{r} = r^{3/2}$. To avoid cluttering of formulae, we will use r instead of \tilde{r} henceforth unless mentioned otherwise. So the coordinate r will parametrise Region 3, and $\tau = \sum \frac{\mathcal{C}_n + i\mathcal{D}_n}{r^n}$.

The above computation was done assuming that $z > (z_i, \tilde{z}_j)$, which at this stage can be guaranteed if we take $\theta_{1,2}$ small. This gives rise to special set of configurations of seven-branes where they are distributed along other angular directions. However one might get a little worried if there exists some $\tilde{z}_j \equiv \tilde{z}_o$ related to the *farthest* seven-brane(s) where the above approximation fails to hold. This can potentially happen when we try to compute the mass of the heaviest quark in our theory. The question is whether we can still use the τ derived in (2.33), or we need to modify the whole picture.

Before we go into answering this question, the choice of z bigger than (z_i, \tilde{z}_j) already needs more convincing elaboration because allowing $\theta_{1,2}$ small is a rather naive argument. The situation at hand is more subtle than that and, as we will argue below, the picture that we have right now is incomplete.

To get the full picture, observe first that z being given by our embedding equation (2.8), means that if we want to be in Region 3, we need to specify the condition $r > r_0$ in the definition of z . This way a given z will always imply points in Region 3 for varying choices of the angular coordinates (θ_i, ϕ_i, ψ) . However similar argument cannot be given for any choices of (z_i, \tilde{z}_j) . A particular choice of (z_i, \tilde{z}_j) may imply very large r with small angular choices or small r with large angular choices. Thus

analysing the system only in terms of the r coordinate is tricky. In terms of the full complex coordinates, $z > (z_i, \tilde{z}_j)$ would mean that we are always looking at points away from the surfaces given by $z = z_i$ and $z = \tilde{z}_j$.

What happens when we touch the $z = z_i$ surfaces? For these cases $F(z_i) \rightarrow 0$ and therefore we are no longer in the weak coupling regime. For all $F(z_i) = 0$ imply $j(\tau) \rightarrow 0$ which in turn means $\tau = \exp(i\pi/3)$ on these surfaces. These are the constant coupling regimes of [28] where the string couplings on these surfaces are *not* weak. On the other hand, near any one of the seven-branes $z = \tilde{z}_j$ we are in the weak coupling regimes and so (2.33) will imply

$$\tau(z) = \frac{1}{2\pi i} \log(z - \tilde{z}_j) \rightarrow i\infty \quad (2.34)$$

which of course is expected but nevertheless problematic for us. This is because we need logarithmic behavior of axio-dilaton in Region 2, but not in Region 3. For a good UV behavior, we need axio-dilaton to behave like (2.33) everywhere in Region 3.

In addition to that there is also the issue of the heaviest quarks creating additional log divergences that we mentioned earlier. These seven branes are located at $z = \tilde{z}_j \equiv \tilde{z}_o$, and therefore if we can make the axio-dilaton independent of the coordinates \tilde{z}_o then at least we won't get any divergences from these seven-branes. It turns out that there are configurations (or rearrangements) of seven-brane(s) that allow us to do exactly that. To see one such configuration, let us define $F(z), G(z)$ and $\Delta(z)$ in (2.32) in the following way:

$$\begin{aligned} F(z) &= (z - \tilde{z}_o) \prod_{i=1}^7 (z - z_i), & G(z) &= (z - \tilde{z}_o)^2 \prod_{i=1}^{10} (z - \hat{z}_i) \\ \Delta(z) &= (z - \tilde{z}_o)^3 \prod_{j=1}^{21} (z - \tilde{z}_j) \end{aligned} \quad (2.35)$$

which means that we are stacking a bunch of *three* seven-branes at the point $z = \tilde{z}_o$, and

$$\prod_{j=1}^{21} (z - \tilde{z}_j) \equiv 4 \prod_{i=1}^7 (z - z_i)^3 + 27(z - \tilde{z}_o) \prod_{i=1}^{10} (z - \hat{z}_i)^2 \quad (2.36)$$

implying that the axio-dilaton τ becomes independent of \tilde{z}_o and behaves exactly as in (2.33) with (i, j) in (2.33) varying upto (7, 21) respectively.

The situation is now getting better. We have managed to control a subset of log divergences. To get rid of the other set of log divergences that appear on the remaining twenty-one surfaces, one possible way would be to modify the embedding (2.8). Recall that our configuration is non-supersymmetric and therefore we are not

required to use the embedding (2.8). In fact a change in the embedding equation will also explain the axio-dilaton choice (2.25) of Region 2. To change the embedding equation (2.8) we will use similar trick that we used to kill off the three-form fluxes, namely, attach anti-branes. These anti seven-branes¹⁶ are embedded via the following equation:

$$r^{3/2} e^{i(\psi - \phi_1 - \phi_2)} \sin \frac{\theta_1}{2} \sin \frac{\theta_2}{2} = r_0 e^{i\Theta} \quad (2.37)$$

where Θ is some angular parameter, and could vary for different anti seven-branes. The above embedding will imply that their overlaps with the corresponding seven-branes are only partial¹⁷. And since we require

$$|\tilde{z}_j|^{2/3} < r_o$$

it will appear effectively that we can only have seven-branes in Regions 1 and 2, and *bound* states of seven-branes and anti seven-branes in Region 3.¹⁸ This way the axio-dilaton in Region 3 will indeed behave as (2.33) for all z (except for the above mentioned seven points).

There are two loose ends that we need to tie up to complete this side of the story. The first one is the issue of Gauss' law, or more appropriately, charge conservation. The original configuration of 24 seven branes had zero global charge, but now with the addition of anti seven-branes charge conservation seems to be problematic. There are a few ways to resolve this issue. First, we can assume that that branes wrap topologically trivial cycles, much like the ones of [17]. Then charge conservation is automatic. The second alternative is to isolate six seven-branes using some appropriate F and G functions, so that they are charge neutral. This is of course one part of the constant coupling scenario of [29]. Now if we make the (θ_2, ϕ_2) directions non-compact then we can put in a configuration of 18 seven-branes and anti seven-branes pairs together using the embeddings (2.8) and (2.37) respectively. The system would look effectively like what we discussed above. Since the whole system is now charge neutral, compactification shouldn't be an issue here.

The second loose end is the issue of tachyons between the seven-brane and anti seven-brane pairs. Again, as for the anti-D5 branes and D7-brane case [26], switching on appropriate electric and magnetic fluxes will make the tachyon massless! Therefore the system will be stable and would behave exactly as we wanted, namely, the axio-dilaton will not have the log divergences over any slices in Region 3.

¹⁶They involve both local and non-local anti seven-branes.

¹⁷For example if we have a seven-brane at $z = \tilde{z}_1$ such that lowest point of the seven brane is $r = |\tilde{z}_1|^{2/3} < r_o$, then the corresponding anti-brane has only partial overlap with this.

¹⁸Of course this effective description is only in terms of the axio-dilaton charges. In terms of the embedding equation for the seven-branes (2.8) this would imply that we can define z with $r > r_o$ and \tilde{z}_j with $r < r_o$.

This behavior of axio-dilaton justifies the $r^{-\epsilon(\alpha)}$ in (2.25) in Region 2. So the full picture would be a set of seven-branes with electric and magnetic fluxes embedded via (2.8) and another set of anti seven-branes embedded via (2.37) lying completely in Region 3.

Thus in Region 3 both the three-forms vanish and therefore $g_1 = g_2 = g_{\text{YM}}$ with g_1, g_2 being the couplings for $SU(N + M), SU(N + M)$. From (2.2) we can compute the β -function for g_{YM} as:

$$\beta(g_{\text{YM}}) \equiv \frac{\partial g_{\text{YM}}}{\partial \log \Lambda} = \frac{g_{\text{YM}}^3}{16\pi} \sum_{n=1}^{\infty} \frac{n \mathcal{D}_n}{\Lambda^n} \quad (2.38)$$

where Λ is the usual RG scale related to the radial coordinate in the supergravity approximation. For $\Lambda \rightarrow \infty$, $\beta(g_{\text{YM}}) \rightarrow 0$ implying a conformal theory in the far UV. We can fix the 't Hooft coupling to be strong to allow for the supergravity approximation to hold consistently at least for all points away from the $z = z_i, i = 1, \dots, 7$ surfaces.

Existence of axio-dilaton τ of the form (2.33) and the seven-brane sources will tell us, from (2.27), that the unwarped metric may not remain Ricci flat. For example it is easy to see that

$$\tilde{\mathcal{R}}_{rr} = \frac{\mathcal{A}_{\mathcal{D}}}{r^2 \mathcal{D}_0^2} \sum_{n,m=1}^{\infty} nm \frac{(\mathcal{C}_n + i\mathcal{D}_n)(\mathcal{C}_m - i\mathcal{D}_m)}{r^{n+m}} + \mathcal{O}\left(\frac{1}{r^n}\right) \quad (2.39)$$

where the last term should come from the seven-brane sources and, because of these sources, we don't expect $\tilde{\mathcal{R}}_{rr}$ to vanish to lowest order in $g_s N_f$.¹⁹ The term $\mathcal{A}_{\mathcal{D}}$ is given by the following infinite series:

$$\mathcal{A}_{\mathcal{D}} = 1 - \sum_{k,l=1}^{\infty} \frac{\mathcal{D}_k \mathcal{D}_l \mathcal{D}_0^{-2}}{r^{k+l}} + \sum_{k,l,p,q=1}^{\infty} \frac{\mathcal{D}_k \mathcal{D}_l \mathcal{D}_p \mathcal{D}_q \mathcal{D}_0^{-2}}{r^{k+l+p+q}} + \dots \quad (2.40)$$

Similarly one can show that

$$\tilde{\mathcal{R}}_{ab} = \frac{\mathcal{A}_{\mathcal{D}}}{\mathcal{D}_0^2} \sum_{n,m=0}^{\infty} \frac{(\partial_a \mathcal{C}_n + i\partial_a \mathcal{D}_n)(\partial_b \mathcal{C}_m - i\partial_b \mathcal{D}_m)}{r^{n+m}} + \mathcal{O}\left(\frac{1}{r^n}\right) \quad (2.41)$$

for $(a, b) \neq r$. For $\tilde{\mathcal{R}}_{rb}$ similar inverse r dependence can be worked out. In the far UV we expect the unwarped curvatures should be equal to the AdS curvatures. The warp factor h on the other hand can be determined from the following variant of (2.28):

$$d * dh^{-1} = \kappa_{10}^2 \text{tr} (F^{(1)} \wedge F^{(1)} - \mathcal{R} \wedge \mathcal{R}) \Delta_2(z) + \dots \quad (2.42)$$

¹⁹Although, as discussed before, the deviation from Ricci flatness will be very small.

because we expect no non-zero three-forms in Region 3. The dotted terms are the non-abelian corrections from the seven-branes. As r is increased i.e $r \gg r_0$, we expect $F^{(1)}$ to fall-off (recall that they appear from the anti (1,1) five-branes located in the neighborhood of $r = r_0$) and therefore can be absorbed in \mathcal{R} . Once we embed the seven-brane gauge connection in some part of spin-connection, we expect

$$\square h^{-1} = \mathcal{O}\left(\frac{1}{r^n}\right) \quad (2.43)$$

from the non-abelian corrections via pull-backs. Solving this will reproduce the generic form for h :

$$h = \frac{L^4}{r^4} \left[1 + \sum_{i=1}^{\infty} \frac{a_i(\psi, \theta_i, \phi_i)}{r^i} \right] \quad (2.44)$$

with a constant L^4 and a_i 's are suppressed by powers of $g_s N_f$. More details on this is given in the **Appendix A** and **B**. At far UV we recover the AdS picture implying a strongly coupled conformal behavior in the dual gauge theory.

From the above discussion we can conclude that the warp factor and the axio-dilaton will have the inverse r behavior. We will use this background to do the Wilson loop computation in the next section.

3. Heavy Quark Potential from Gravity

Before we go into the actual computation of the Wilson loop, let us point out some generic standard arguments that map the Wilson loop computation to the string action and then to the quark anti-quark potential.

Consider the Wilson loop of a rectangular path \mathcal{C} with spacelike width d and timelike length T . The timelike paths can be thought of as world lines of pair of quarks $Q\bar{Q}$ separated by a spatial distance d . Studying the expectation value of the Wilson loop in the limit $T \rightarrow \infty$, one can show that it behaves as

$$\langle W(\mathcal{C}) \rangle \sim \exp(-TE_{Q\bar{Q}}) \quad (3.1)$$

where $E_{Q\bar{Q}}$ is the energy of the $Q\bar{Q}$ pair which we can identify with their potential energy $V_{Q\bar{Q}}(d)$ as the quarks are static. At this point we can use the principle of holography [9] [10] [30] and identify the expectation value of the Wilson loop with the exponential of the *renormalised* Nambu-Goto action,

$$\langle W(\mathcal{C}) \rangle \sim \exp(-S_{\text{NG}}^{\text{ren}}) \quad (3.2)$$

with the understanding that \mathcal{C} is now the boundary of string world sheet. Note that we are computing Wilson loop of gauge theory living on flat four dimensional space-time $x^{0,1,2,3}$. Whereas the string worldsheet is embedded in curved five-dimensional

manifold with coordinates $x^{0,1,2,3}$ and r . We will identify the five-dimensional manifold with Region 3 that we discussed above.

To be consistent with the recipe in [10], we need to make sure that the induced four dimensional metric at the boundary of the string world sheet \mathcal{C} is flat. For an AdS space, this is guaranteed as long as the world sheet ends on boundary of AdS space where the induced four dimensional metric can indeed be written as $\eta_{\mu\nu}$. Using the geometry constructed in the previous section for Region 3, we see that the metric is asymptotically AdS and therefore induces a flat Minkowski metric at the boundary via:

$$\lim_{u \rightarrow 0} u^2 g_{\mu\nu} = \eta_{\mu\nu} \quad (3.3)$$

where $u = r^{-1}$ and $g_{\mu\nu}$ is the full metric (including the warp factor) in Region 3. Thus we can make the identification (3.2). Once this subtlety is resolved, comparing (3.1) and (3.2) we can read off the potential

$$V_{Q\bar{Q}} = \lim_{T \rightarrow \infty} \frac{S_{\text{NG}}^{\text{ren}}}{T} \quad (3.4)$$

Thus knowing the renormalised string world sheet action, we can compute $V_{Q\bar{Q}}$ for a strongly coupled gauge theory.

The above discussion was all for gauge theory at zero temperature. What happens when we allow non-zero temperatures? Does the above identification (3.4) between the quark anti-quark potential and the renormalised Nambu-Goto action go through again?

The answer is yes, but the derivation is a little more subtle than what we presented for the zero temperature case. At high temperatures and density we expect the medium effects to *screen* the interaction between the heavy quark and anti-quark pairs. The resulting effective potential between the quark anti-quark pairs separated by a distance d at temperature \mathcal{T} can then be expressed succinctly in terms of the free energy $F(d, \mathcal{T})$, which generically takes the following form:

$$F(d, \mathcal{T}) = \sigma d f_s(d, \mathcal{T}) - \frac{\alpha}{d} f_c(d, \mathcal{T}) \quad (3.5)$$

where σ is the string tension, α is the gauge coupling and f_c and f_s are the screening functions²⁰ (see for example [31] and references therein). For the quark and the anti-quark pair kept at $+\frac{d}{2}$ and $-\frac{d}{2}$ we expect the Wilson lines $W(\pm\frac{d}{2})$ to be related to the free energy via:

$$\exp\left[-\frac{F(d, \mathcal{T})}{\mathcal{T}}\right] = \frac{\langle W^\dagger(+\frac{d}{2}) W(-\frac{d}{2}) \rangle}{\langle W^\dagger(+\frac{d}{2}) \rangle \langle W(-\frac{d}{2}) \rangle} \quad (3.6)$$

²⁰We expect the screening functions f_s, f_c to equal identity when the temperature goes to zero. This gives the zero temperature Cornell potential.

In terms of Wilson loop, the free energy (3.5) is now related to the renormalised Nambu-Goto action for the string on a background with a black-hole²¹. One may also note that the theory we get is a four-dimensional theory *compactified* on a circle in Euclideanised version and not a three-dimensional theory.

3.1 Computing the Nambu-Goto Action: Zero Temperature

Our first attempt to compute the NG action would be to consider the zero temperature case. This means that we make the black-hole factors g_i in (2.11) to be identity. The string configuration that we will take to do the required computation is given below in Figure 6. Note that we have configured our geometry such that the string is exclusively in Region 3. We will provide a stronger motivation for this soon. For the time being observe that the configuration in Figure 6 has one distinct advantage over all other configurations studied in the literature, namely, that because of the absence of three-forms in Region 3 we will not have the UV divergence of the Wilson loop attributed to the logarithmically varying B field [23]. In fact even if the string enters Regions 2 and 1 we will not encounter any problems because there are no UV three-forms in our model.

Since the system is not dynamical, the world line for the static $Q\bar{Q}$ can be chosen to be

$$x^1 = \pm \frac{d}{2}, \quad x^2 = x^3 = 0 \quad (3.7)$$

and using $u \equiv 1/r$ we can rewrite the metric in Region 3 as²²:

$$ds^2 = g_{\mu\nu} dX^\mu dX^\nu = \mathcal{A}_n(\psi, \theta_i, \phi_i) u^{n-2} [-g(u) dt^2 + d\vec{x}^2] \\ + \frac{\mathcal{B}_l(\psi, \theta_i, \phi_i) u^l}{\mathcal{A}_m(\psi, \theta_i, \phi_i) u^{m+2} g(u)} du^2 + \frac{1}{\mathcal{A}_n(\psi, \theta_i, \phi_i) u^n} ds_{\mathcal{M}_5}^2 \quad (3.8)$$

where \mathcal{A}_n are the coefficients that can be extracted from the a_i in (2.44), the black hole factor $g(u) = 1$ for the zero-temperature case, and $ds_{\mathcal{M}_5}^2$ is the metric of the internal space that includes the corrections given in (2.41). This can be made precise as

$$\frac{1}{\sqrt{h}} = \frac{1}{L^2 u^2 \sqrt{a_i u^i}} \equiv \mathcal{A}_n u^{n-2} = \frac{1}{L^2 u^2} \left[a_0 - \frac{a_1 u}{2} + \left(\frac{3a_1^2}{8a_0} - \frac{a_2}{2} \right) u^2 + \dots \right] \quad (3.9)$$

giving us $\mathcal{A}_0 = \frac{a_0}{L^2}$, $\mathcal{A}_1 = -\frac{a_1}{2L^2}$, $\mathcal{A}_2 = \frac{1}{L^2} \left(\frac{3a_1^2}{8a_0} - \frac{a_2}{2} \right)$ and so on. Note that since a_i , $i \geq 1$ are of $\mathcal{O}(g_s N_f)$ and $L^2 \propto \sqrt{g_s N}$, all \mathcal{A}_i are very small. The r^{-n} corrections along the radial direction given in (2.39) are accommodated above via $\mathcal{B}_l u^l$ series.

²¹There is a big literature on the subject where quark anti-quark potential has been computed using various different approaches like pNRQCD [32], hard wall AdS/CFT [33, 34] and other techniques [20, 21]. Its reassuring to note that the results that we get using our newly constructed background matches very well with the results presented in the above references. This tells us that despite the large N nature there is an underlying universal behavior of the confining potential.

²²We will be using the Einstein summation convention henceforth unless mentioned otherwise.

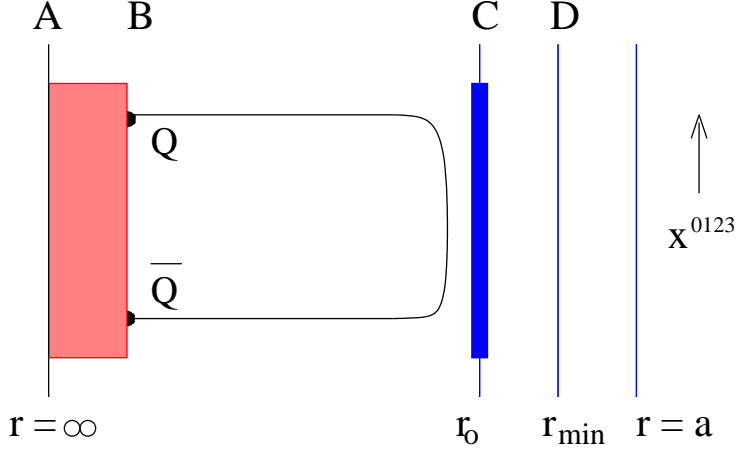


Figure 6: The string configuration that we will use to evaluate the Wilson loop in the dual gauge theory. The line A determines the actual boundary, with the line B denoting the extent of the seven brane. We will assume that line B is very close to the line A . The line C at $r = r_o$ denotes the boundary between Region 3 and Region 2. Region 2 is the interpolating region that ends at $r = r_{\min}$. At the far IR the geometry is cut-off at $r = a$ from the blown-up S^3 . As discussed in the text, the string has a maximum dip that will eventually lead to the confining potential between the heavy quark and the antiquark.

Now suppose $X^\mu : (\sigma, \tau) \rightarrow (x^{0123}, u, \psi, \phi_i, \theta_i)$ is a mapping from string world sheet to space-time. Choosing a parametrization $\tau = x^0 \equiv t, \sigma = x^1 \equiv x$ with the boundary of the world sheet embedding being the path \mathcal{C} , we see that we can have

$$\begin{aligned} X^0 &= t, & X^1 &= x, & X^2 &= X^3 = 0, & X^7 &= u(x), & X^6 &= \psi = 0 \\ (X^4, X^5) &= (\theta_1, \phi_1) = (\pi/2, 0), & (X^8, X^9) &= (\theta_2, \phi_2) = (\pi/2, 0) \end{aligned} \quad (3.10)$$

which is almost like the slice (2.15) that we choose in [13]. The advantage of such a choice is to get rid of the awkward angular variables that appear for our background so that we will have only a r (or u) dependent background like in (2.16) discussed before. We will also impose the boundary condition

$$u(\pm d/2) = u_\gamma \approx 0 \quad (3.11)$$

where u_γ denote the position of the seven brane *closest* to the boundary. The Nambu-Goto action for the string connecting this seven brane is:

$$\begin{aligned} S_{\text{string}} &= \frac{T_0}{2\pi} \int d\sigma d\tau \left[\sqrt{-\det [(g_{\mu\nu} + \partial_\mu \phi \partial_\nu \phi) \partial_a X^\mu \partial_b X^\nu]} + \frac{1}{2} \epsilon^{ab} B_{ab} + J(\phi) \right. \\ &\quad \left. + \epsilon^{ab} \partial_a X^m \partial_b X^n \bar{\Theta} \Gamma_m \Gamma^{abc\dots} \Gamma_n \Theta F_{abc\dots} + \mathcal{O}(\Theta^4) \right] \end{aligned} \quad (3.12)$$

where $a, b = 1, 2$, $\partial_1 \equiv \frac{\partial}{\partial \tau}$, $\partial_2 \equiv \frac{\partial}{\partial \sigma}$. The other fields appearing in the action are the pull backs of the NS B field B_{ab} , the dilaton coupling $J(\phi)$ and the RR field

strengths F_{abc} . It's clear that once we switch off the fermions i.e. $\Theta = \bar{\Theta} = 0$ the RR fields decouple. The B_{NS} field does couple to the fundamental string but as we discussed before, in Region 3 we don't expect to see any three-form field strengths. This is because the amount of B_{NS} that could leak out from Region 2 to Region 3 is:

$$B_{NS} = M\mathcal{S}[1 - f(r)] = M\mathcal{S} e^{-\alpha(r-r_0)}, \quad r > r_0 \quad (3.13)$$

where \mathcal{S} is the two-form:

$$\begin{aligned} \mathcal{S} = & g_s \left(b_1(r) \cot \frac{\theta_1}{2} d\theta_1 + b_2(r) \cot \frac{\theta_2}{2} d\theta_2 \right) \wedge e_\psi - \frac{g_s b_4(r)}{12\pi} \sin \theta_2 d\theta_2 \wedge d\phi_2 \quad (3.14) \\ & + \frac{3g_s}{4\pi} \left[\left(1 + g_s N_f - \frac{1}{r^{2g_s N_f}} + \frac{9a^2 g_s N_f}{r^2} \right) \log \left(\sin \frac{\theta_1}{2} \sin \frac{\theta_2}{2} \right) + b_3(r) \right] \sin \theta_1 d\theta_1 \wedge d\phi_1 \\ & - \frac{g_s}{12\pi} \left(2 - \frac{36a^2 g_s N_f}{r^2} + 9g_s N_f - \frac{1}{r^{16g_s N_f}} - \frac{1}{r^{2g_s N_f}} + \frac{9a^2 g_s N_f}{r^2} \right) \sin \theta_2 d\theta_2 \wedge d\phi_2 \end{aligned}$$

and b_n have been defined before. We see that not only B_{NS} has an inverse r fall off, but also has a strong exponential decay because $\alpha \gg 1$. This is the main reason why there are no NS or RR three-forms in Region 3, making our computation of the Wilson loop relatively easier compared to the pure Klebanov-Strassler case.

On the other hand dilaton will couple *additionally* via the $J(\phi)$ term. Although this coupling of ϕ is not to the X^μ , we can still control this coupling by arranging the other seven-branes such that:

$$\text{Re} \left(\sum_{i=1}^{n_1} \frac{3z_i^n}{z^n} - \sum_{j=1}^{n_2} \frac{\tilde{z}_j^n}{z^n} \right) < \epsilon \quad \text{for } 0 \leq n \leq m_o \quad (3.15)$$

with ϵ very small and m_o a sufficiently big number. Under this condition the dilaton will be essentially constant and the axio-dilaton τ would behave as:

$$\tau = \tau_0 + \sum_{n=1}^{\infty} \frac{\mathcal{C}_n}{r^n} + i \sum_{n>m_o}^{\infty} \frac{\mathcal{D}_n}{r^n} \quad (3.16)$$

so that its contribution to NG action can be ignored although the $\mathcal{B}_l u^l$ contribution still dominates, because the seven-branes continue to affect the geometry from their energy-momentum tensors and the axion charges. In this limit both string and Einstein frame metrics are identical and the background dilaton is

$$\phi = \log g_s - g_s \mathcal{D}_{n+m_o} u^{n+m_o} + \mathcal{O}(g_s^2) \quad (3.17)$$

which, in the limit $g_s \rightarrow 0$, will be dominated by the constant term (note that m_o is fixed). Because of this form, the NG string will see a slightly different background metric as evident from (3.12).

Thus once the dust settles, using the metric (3.8) with the embedding X^μ given by (3.10), one can easily show that at zero temperature the NG action is given by:

$$S_{\text{NG}} = \frac{T}{2\pi} \int_{-\frac{d}{2}}^{+\frac{d}{2}} \frac{dx}{u^2} \sqrt{\left(\mathcal{A}_n u^n\right)^2 + \left[\mathcal{B}_m u^m + 2g_s^2 \tilde{\mathcal{D}}_{n+m_o} \tilde{\mathcal{D}}_{l+m_o} \mathcal{A}_k u^{n+l+k+2m_o} + \mathcal{O}(g_s^4)\right] \left(\frac{\partial u}{\partial x}\right)^2} \quad (3.18)$$

where we have used $\int dt = T/T_0 \equiv T$ (with $T_0 \equiv 1$ henceforth), $\tilde{\mathcal{D}}_{n+m_o} = (n + m_o)\mathcal{D}_{n+m_o}$; and $\mathcal{A}_n, \mathcal{B}_n$ and \mathcal{D}_{n+m_o} are now defined for choices of the angular coordinates given in (3.10). The above action can be condensed if we redefine:

$$\mathcal{B}_m u^m + 2g_s^2 \tilde{\mathcal{D}}_{n+m_o} \tilde{\mathcal{D}}_{l+m_o} \mathcal{A}_k u^{n+l+k+2m_o} + \mathcal{O}(g_s^4) \equiv \mathcal{G}_l u^l \quad (3.19)$$

which would mean that the constraint equation i.e $\partial_1 T_1^1 = 0$, T_1^1 being the stress-tensor, for $u(x)$ derived from the action (3.18) using (3.19) can be written as

$$\frac{d}{dx} \left(\frac{(\mathcal{A}_n u^n)^2}{u^2 \sqrt{(\mathcal{A}_m u^m)^2 + \mathcal{G}_m u^m \left(\frac{\partial u}{\partial x}\right)^2}} \right) = 0 \quad (3.20)$$

implying that:

$$\frac{(\mathcal{A}_n u^n)^2}{u^2 \sqrt{(\mathcal{A}_m u^m)^2 + \mathcal{G}_m u^m u'(x)^2}} = C_o \quad (3.21)$$

where C_o is a constant, and $u'(x) \equiv \frac{\partial u}{\partial x}$. This constant C_o can be determined in the following way: as we have the endpoints of the string at $x = \pm d/2$, by symmetry the string will be U shaped and if u_{max} is the maximum value of u , we can define $u(0) = u_{\text{max}}$ and $u'(x=0) = 0$. Plugging this in (3.21) we get:

$$C_o = \frac{\mathcal{A}_n u_{\text{max}}^n}{u_{\text{max}}^2} \quad (3.22)$$

Once we have C_o , we can use (3.20) to get the following simple differential equation:

$$\frac{du}{dx} = \pm \frac{1}{C_o \sqrt{\mathcal{G}_m u^m}} \left[\frac{(\mathcal{A}_n u^n)^4}{u^4} - C_o^2 (\mathcal{A}_m u^m)^2 \right]^{1/2} \quad (3.23)$$

which in turn can be used to write $x(u)$ as:

$$x(u) = C_o \int_{u_{\text{max}}}^u dw \frac{w^2 \sqrt{\mathcal{G}_m w^m}}{(\mathcal{A}_n w^n)^2} \left[1 - \frac{C_o^2 w^4}{(\mathcal{A}_m w^m)^2} \right]^{-1/2} \quad (3.24)$$

where we have used $x(u_{\text{max}}) = 0$. Now using the boundary condition given in (3.11) i.e $x(u = u_\gamma) = d/2$, and defining $w = u_{\text{max}} v$, $\epsilon_o = \frac{u_\gamma}{u_{\text{max}}}$ we have

$$d = 2u_{\text{max}} \int_{\epsilon_o}^1 dv v^2 \frac{\sqrt{\mathcal{G}_m u_{\text{max}}^m v^m} (\mathcal{A}_n u_{\text{max}}^n)}{(\mathcal{A}_m u_{\text{max}}^m v^m)^2} \left[1 - v^4 \left(\frac{\mathcal{A}_n u_{\text{max}}^n}{\mathcal{A}_m u_{\text{max}}^m v^m} \right)^2 \right]^{-1/2} \quad (3.25)$$

At this stage we can assume all $\mathcal{A}_n > 0$. This is because for $\mathcal{A}_n > 0$ we can clearly have degrees of freedom in the gauge theory growing towards UV, which is an expected property of models with RG flows. Of course this is done to simplify the subsequent analyses. Keeping \mathcal{A}_n arbitrary will also allow us to derive the linear confinement behavior, but this case will require a more careful analysis. We will leave this for future works. Note also that similar behavior is seen for the the Klebanov-Strassler model, and we have already discussed how degrees of freedom run in Regions 2 and 3. Another obvious condition is that d , which is the distance between the quarks, cannot be imaginary. From (3.25) we can see that the integral becomes complex for

$$\mathcal{F}(v) \equiv v^4 \left(\frac{\mathcal{A}_n u_{\max}^n}{\mathcal{A}_m u_{\max}^m v^m} \right)^2 > 1 \quad (3.26)$$

whereas for $\mathcal{F}(v) = 1$ the integral becomes singular. Then for d to be always real we must have

$$\mathcal{F}(v) \leq 1 \quad (3.27)$$

We can now use, without loss of generality, $\mathcal{A}_0 = 1$ and $\mathcal{A}_1 = 0$ in units of L^2 . Such a choice is of course consistent with supergravity solution for our background (as evident from (3.9)). Therefore analyzing the condition (3.27), one easily finds that we must have

$$\frac{1}{2}(m+1)\mathcal{A}_{m+3} u_{\max}^{m+3} \leq 1 \quad (3.28)$$

for d to be real. This condition puts an upper bound on u_{\max} and we can use this to constrain the fundamental string to lie completely in Region 3 as depicted in Figure 5 earlier. Observe that for AdS spaces, $\mathcal{A}_n = 0$ for $n > 0$ and hence there is no upper bound for u_{\max} . This is also the main reason why we see confinement using our background but not from the AdS backgrounds. Furthermore one might mistakenly think that generic Klebanov-Strassler background should show confinement because the space is physically cut-off due to the presence of a blown-up S^3 . Although such a scenario implies a u_{\max} for the fundamental string, this doesn't naturally lead to confinement because due to the presence of logarithmically varying B_{NS} fields there are UV divergences of the Wilson loop. These divergences *cannot* be removed by simple regularization schemes [23].

Coming back to (3.18) we see that it can be further simplified. Using (3.21), (3.22) and (3.23) in (3.18), we can write it as an integral over u :

$$\begin{aligned} S_{\text{NG}} &= \frac{T}{\pi} \int_{u_\gamma}^{u_{\max}} \frac{du}{u^2} \sqrt{\mathcal{G}_l u^l} \left[1 - \frac{C_o^2 u^4}{(\mathcal{A}_m u^m)^2} \right]^{-1/2} \\ &= \frac{T}{\pi} \frac{1}{u_{\max}} \int_{\epsilon_o}^1 \frac{dv}{v^2} \sqrt{\mathcal{G}_m u_{\max}^m v^m} \left[1 - v^4 \left(\frac{\mathcal{A}_n u_{\max}^n}{\mathcal{A}_m u_{\max}^m v^m} \right)^2 \right]^{-1/2} \end{aligned} \quad (3.29)$$

where in the second equality we have taken $v = u/u_{\max}$.

This simplified action (3.29) is not the full story. It is also divergent in the limit $\epsilon_o \rightarrow 0$. We isolate the divergent part of the above integral (3.29) by first computing it as a function of ϵ_o . The result is

$$S_{\text{NG}} \equiv S_{\text{NG}}^{\text{I}} + S_{\text{NG}}^{\text{II}} = \frac{T}{\pi} \frac{1}{u_{\max}} \int_{\epsilon_o}^1 \frac{dv}{v^2} \sqrt{\mathcal{G}_m u_{\max}^m v^m} + \frac{T}{\pi} \frac{1}{u_{\max}} \int_{\epsilon_o}^1 \frac{dv}{v^2} \sqrt{\mathcal{G}_m u_{\max}^m v^m} \left\{ \left[1 - v^4 \left(\frac{\mathcal{A}_n u_{\max}^n}{\mathcal{A}_m u_{\max}^m v^m} \right)^2 \right]^{-1/2} - 1 \right\} \quad (3.30)$$

Now by expanding $\sqrt{\mathcal{G}_m u_{\max}^m v^m} = \tilde{\mathcal{G}}_l v^l$ we can compute the first integral to be

$$S_{\text{NG}}^{\text{I}} = \frac{T}{\pi} \frac{1}{u_{\max}} \left(-\tilde{\mathcal{G}}_0 + \frac{\tilde{\mathcal{G}}_0}{\epsilon_o} + \sum_{l=2} \frac{\tilde{\mathcal{G}}_l}{l-1} + \mathcal{O}(\epsilon_o) + \dots \right) \quad (3.31)$$

where $\tilde{\mathcal{G}}_0 = \mathcal{G}_0$, $\tilde{\mathcal{G}}_1 = \frac{1}{2} \mathcal{G}_1 u_{\max}$ and so on. The second integral becomes

$$S_{\text{NG}}^{\text{II}} = \frac{T}{\pi} \frac{1}{u_{\max}} \int_0^1 \frac{dv}{v^2} \sqrt{\mathcal{G}_m u_{\max}^m v^m} \left\{ \left[1 - v^4 \left(\frac{\mathcal{A}_n u_{\max}^n}{\mathcal{A}_m u_{\max}^m v^m} \right)^2 \right]^{-1/2} - 1 \right\} + \mathcal{O}(\epsilon_o^3) \quad (3.32)$$

where the ϵ_o dependence here appears to $\mathcal{O}(\epsilon_o^3)$; and we have set $\mathcal{G}_1 = 0$ without loss of generality. Now combining the result in (3.31) and (3.32), we can obtain the renormalized action by subtracting the divergent term $\mathcal{O}(1/\epsilon)$ in the limit $\epsilon_o \rightarrow 0$ and obtain the following result

$$S_{\text{NG}}^{\text{ren}} = \frac{T}{\pi} \frac{1}{u_{\max}} \left\{ -\tilde{\mathcal{G}}_0 + \sum_{l=2} \frac{\tilde{\mathcal{G}}_l}{l-1} - \int_0^1 \frac{dv}{v^2} \sqrt{\mathcal{G}_m u_{\max}^m v^m} + \mathcal{O}(g_s^2) + \int_0^1 \frac{dv}{v^2} \sqrt{\mathcal{G}_m u_{\max}^m v^m} \left[1 - v^4 \left(\frac{\mathcal{A}_n u_{\max}^n}{\mathcal{A}_m u_{\max}^m v^m} \right)^2 \right]^{-1/2} + \mathcal{O}(\epsilon_o) \right\} \quad (3.33)$$

where the third term in (3.33), including the $\mathcal{O}(g_s^2)$ correction, is related to the action for a straight string in this background in the limit $g_s \rightarrow 0$. Our subtraction scheme is more involved because the straight string sees a complicated metric due to the background dilaton and non-Ricci flat unwarped metric. This effect is *independent* of any choice of the warp factor. We expect this action to be finite in the limit $\epsilon_o \rightarrow 0$.

Once we have the action, we should use this to compute the $Q\bar{Q}$ potential through (3.4). Looking at (3.25) we observe that the relation between d and u_{\max} is parametric and can be quite involved depending on the coefficients \mathcal{A}_n . If we have $\mathcal{A}_n = 0, \mathcal{G}_n = 0$

for $n > 0$, we recover the well known AdS result, namely: $d \sim u_{\max}$ and $V_{Q\bar{Q}} \sim \frac{1}{d}$. But in general (3.25) and (3.33) should be solved together to obtain the potential.

As it stands, (3.25) and (3.33) are both rather involved. So to find some correlation between them we need to go to the limiting behavior of u_{\max} . Therefore in the following, we will study the behaviour of d and $S_{\text{NG}}^{\text{ren}}$ for the cases where u_{\max} is large and small.

3.1.1 Quark-Antiquark potential for small u_{\max}

Let us first consider the case where u_{\max} is small. In this limit we can impose $u_\gamma = \epsilon u_{\max}$, so that $\epsilon_o = \epsilon$ in all the above integrals and consequently their lower limits will be independent of u_{\max} . We can also approximate

$$\mathcal{A}_n u_{\max}^n = \mathcal{A}_0 + \mathcal{A}_2 u_{\max}^2 \equiv 1 + \eta \quad (3.34)$$

where $\mathcal{A}_0 = 1$ and $\mathcal{A}_2 u_{\max}^2 = \eta$. Using this we can write both (3.25) and (3.33) as Taylor series in η around $\eta = 0$. The result is

$$\begin{aligned} d &= \sqrt{\eta} [a_0 + a_1 \eta + \mathcal{O}(\eta^2)] \\ S_{\text{NG}}^{\text{ren}} &= \frac{T}{\pi} \left[\frac{b_0 + b_1 \eta + \mathcal{O}(\eta^2)}{\sqrt{\eta}} \right] \end{aligned} \quad (3.35)$$

with a_0, a_1, b_0, b_1 are defined in the following way:

$$\begin{aligned} a_0 &= \frac{2}{\sqrt{\mathcal{A}_2}} \int_0^1 dv \frac{v^2}{\sqrt{1-v^4}} = \frac{1.1981}{\sqrt{\mathcal{A}_2}} \\ a_1 &= \frac{2}{\sqrt{\mathcal{A}_2}} \int_0^1 dv \frac{v^2}{\sqrt{1-v^4}} \left[\frac{1-v^6}{1-v^4} + \left(\frac{\mathcal{G}_2 - 4\mathcal{A}_2}{2\mathcal{A}_2} \right) v^2 \right] \\ b_0 &= \sqrt{\mathcal{A}_2} \left[-1 + \int_0^1 dv \left(\frac{1 - \sqrt{1-v^4}}{v^2 \sqrt{1-v^4}} \right) \right] = -0.62 \sqrt{\mathcal{A}_2} \\ b_1 &= \frac{1}{2\sqrt{\mathcal{A}_2}} \left\{ \mathcal{G}_2 + \int_0^1 dv \left[\frac{2\mathcal{A}_2 v^4 + \mathcal{G}_2 v^2 (1+v^2) (1 - \sqrt{1-v^4})}{v^2 (1+v^2) \sqrt{1-v^4}} \right] \right\} \end{aligned} \quad (3.36)$$

where we have taken $\mathcal{G}_0 = 1$ and $\mathcal{G}_1 = 0$ without loss of generality. Note that all the above integrals are independent of η (or u_{\max}) because all $\mathcal{O}(\epsilon)$ corrections are independent of u_{\max} . Note also that $b_0 = -|b_0|$. In this limit clearly increasing η increases d , the distance between the quarks. For small η , $d = a_0 \sqrt{\eta}$, and therefore the Nambu-Goto action will become:

$$S_{\text{NG}}^{\text{ren}} = T \left[- \left(\frac{a_0 |b_0|}{\pi} \right) \frac{1}{d} + \left(\frac{b_1}{\pi a_0} \right) d + \mathcal{O}(d^3) \right] \quad (3.37)$$

where all the constants have been defined in (3.36). Using (3.4) we can determine the short-distance potential to be (recall $T_0 = 1$):

$$\begin{aligned} V_{Q\bar{Q}} &= -\left(\frac{a_0|b_0|}{\pi}\right)\frac{1}{d} + \left(\frac{b_1}{\pi a_0}\right)d + \mathcal{O}(d^3) \\ &= -\frac{0.236}{d} + (0.174\mathcal{G}_2 + 0.095\mathcal{A}_2)d + \mathcal{O}(d^3) \end{aligned} \quad (3.38)$$

which is dominated by the inverse d behavior, i.e the expected Coulombic behavior. Note that the coefficient of the Coulomb term is independent of the warp factor and therefore should be universal. This result, in appropriate units, is of the same order of magnitude as the real Coulombic term for the Charmonium spectra [31, 35, 32, 34]. This prediction, along with the overall minus sign, should be regarded as a success of our model (see also [36] where somewhat similar results have been derived in a string theory inspired model). The second term on the other hand is model dependent, and vanishes in the pure AdS background.

Note also that the above computations are valid for infinitely massive quark-antiquark pair. For lighter quarks, we expect the results to differ. It would be interesting to compare these results with the ones where quarks are much lighter.

3.1.2 Quark-Antiquark potential for large u_{\max}

To analyse the quark-antiquark potential for large u_{\max} we first define a quantity called $z_{\max} \equiv \tilde{u}_{\max}^{-1}$ which would be our small tunable parameter. We note that the *smallest* z_{\max} will come from the following equality:

$$\frac{1}{2} \sum_m (m+1) \frac{\mathcal{A}_{m+3}}{z_{\max}^{m+3}} = 1 \quad (3.39)$$

which is the upper bound on the inequality (3.28). Furthermore since we demanded $\mathcal{A}_n \geq 0$, the above condition will imply that the coefficients \mathcal{A}_n has to quickly become very small because in the limit $z_{\max} < 1$

$$\lim_{m \rightarrow \infty} \frac{m+1}{z_{\max}^{m+3}} \rightarrow \infty \quad (3.40)$$

which is perfectly consistent with (3.9) because higher \mathcal{A}_n are proportional to higher powers of $g_s N_f$ and therefore strongly suppressed in the limit $g_s N_f \rightarrow 0$. This will also mean that we can retain only few of the \mathcal{A}_n 's to study the potential for small z_{\max} . In fact we will soon give an estimate of the largest n that we should keep in our analysis.

To determine the distance between the quark we can again use (3.24). However we have to be careful about a few subtleties that appear due to our choice of the scale z_{\max} . First of all note that we will use $w = z_{\max}v$ in (3.24). This will immediately

imply that the lower bound of the integral is no longer ϵ that we had in the previous subsection, but it is

$$\frac{u_\gamma}{z_{\max}} = \frac{\epsilon u_{\max}}{z_{\max}} = \tilde{\epsilon} \rightarrow 0 \quad (3.41)$$

where u_{\max} is the lowest value from the inequality (3.24) that we chose in the previous subsection (to avoid clutter we use the same notation). Note that $\tilde{\epsilon}$ is independent of z_{\max} . Using this we can now write the distance d between the quark and the antiquark as:

$$d = 2V_0 z_{\max}^5 \int_{\tilde{\epsilon}}^{1/z_{\max}^2} dv v^2 \frac{\sqrt{\mathcal{G}_m v^m z_{\max}^m}}{(\mathcal{A}_n v^n z_{\max}^n)^2} \left[1 - z_{\max}^8 \frac{V_0^2}{(\mathcal{A}_k v^k z_{\max}^k)^2} \right]^{-1/2} \quad (3.42)$$

where we have defined $V_0 = \mathcal{A}_n z_{\max}^{-n}$ and sum over repeated index is implied as before.

Comparing V_0 with (3.39) we see that V_0 can be made small if $\mathcal{A}_2 \ll 1$ (which is consistent with (3.9) and (3.34)) as all \mathcal{A}_n for $n \geq 3$ are very small. Additionally, from (3.42), the term $z_{\max}^8 V_0^2$ will imply that it will be sufficient to restrict V_0 to the following series:

$$V_0 = 1 + \frac{\mathcal{A}_2}{z_{\max}^2} + \frac{\mathcal{A}_3}{z_{\max}^3} + \frac{\mathcal{A}_4}{z_{\max}^4} \quad (3.43)$$

because \mathcal{A}_5 onwards are very small to consistently maintain the reality of d in (3.42) as well as their $g_s N_f$ dependences from (3.9). This means d in (3.42) can be further simplified to:

$$\begin{aligned} d &= 2V_0 z_{\max}^5 \int_{\tilde{\epsilon}}^{1/z_{\max}^2} dv v^2 \frac{1 - (\mathcal{A}_2 - \frac{1}{2}\mathcal{G}_2) z_{\max}^2 v^2}{\sqrt{1 - z_{\max}^8 V_0^2 + 2z_{\max}^{10} V_0^2 \mathcal{A}_2 v^2}} \quad (3.44) \\ &\approx 2V_0 \left\{ \left(1 + \frac{1}{2} z_{\max}^8 V_0^2 \right) \frac{1}{3z_{\max}} + \left[\frac{1}{2} (\mathcal{G}_2 - 4\mathcal{A}_2) z_{\max}^2 + \frac{1}{4} (\mathcal{G}_2 - 8\mathcal{A}_2) V_0^2 z_{\max}^{10} \right] \frac{1}{5z_{\max}^5} \right\} \end{aligned}$$

Since we have taken both \mathcal{A}_2 as well as \mathcal{B}_2 to be very small, and plugging in the value of V_0 from (3.43) we see that d is dominated mostly by inverse z_{\max} terms, i.e

$$d = \frac{2}{3z_{\max}} \left[1 + \frac{\mathcal{A}_4^2}{2} + \mathcal{O}(\mathcal{A}_n^3) \right] + \frac{2}{3z_{\max}^2} \mathcal{O}(\mathcal{A}_n^2) + \mathcal{O}\left(\frac{1}{z_{\max}^3}\right) \quad (3.45)$$

The renormalised Nambu-Goto action on the other hand takes the following form:

$$\begin{aligned} S_{\text{NG}}^{\text{ren}} &= \frac{T}{\pi z_{\max}} \int_0^{1/z_{\max}^2} \frac{dv}{v^2} \sqrt{\mathcal{G}_l z_{\max}^l v^l} \left[\left(1 - z_{\max}^8 \frac{V_0^2}{(\mathcal{A}_k v^k z_{\max}^k)^2} \right)^{-1/2} - 1 \right] \\ &\quad + \frac{T}{\pi z_{\max}} \left[-z_{\max}^2 + \frac{\mathcal{G}_2}{2} + \frac{\mathcal{G}_3}{4} \frac{1}{z_{\max}} + \frac{8\mathcal{G}_4 - \mathcal{G}_2^2}{48} \frac{1}{z_{\max}^2} + \dots \right] \quad (3.46) \\ &\approx -\frac{T}{2\pi} (2 + \mathcal{A}_4^2) z_{\max} - \frac{T\mathcal{A}_4^2}{2\pi} \left[2\mathcal{A}_2 - \mathcal{G}_2 \left(\frac{\mathcal{A}_3^2}{\mathcal{A}_4^2} + 2\frac{\mathcal{A}_2}{\mathcal{A}_4} \right) - \frac{\mathcal{G}_2}{\mathcal{A}_4^2} \right] \frac{1}{z_{\max}} + \mathcal{O}\left(\frac{1}{z_{\max}^2}\right) \end{aligned}$$

where it's clear that the string action is dominated by the inverse z_{\max} terms. Now substituting (3.45) and (3.46) in (3.4), we get

$$V_{Q\bar{Q}} = \frac{3\mathcal{A}_4^2}{4\pi} \left[2\mathcal{A}_2 - \mathcal{G}_2 \left(\frac{\mathcal{A}_3^2}{\mathcal{A}_4^2} + 2\frac{\mathcal{A}_2}{\mathcal{A}_4} \right) - \frac{\mathcal{G}_2}{\mathcal{A}_4^2} + \dots \right] d + \mathcal{O}\left(\frac{1}{d}\right) \quad (3.47)$$

which is the required linear potential between the quark and the antiquark. The above potential can also be rewritten as:

$$V_{Q\bar{Q}} = \left(\frac{\mathcal{H}_n \alpha_{\max}^n}{\pi \alpha_{\max}^2} \right) d + \mathcal{O}\left(\frac{1}{d}\right) \quad (3.48)$$

where $\alpha_{\max} \equiv \frac{1}{\mathcal{A}_4}$ and $\mathcal{H}_0 = \frac{3\mathcal{A}_2}{2}$, $\mathcal{H}_1 = -\frac{3\mathcal{A}_2\mathcal{G}_2}{2}$, $\mathcal{H}_2 = -\frac{3\mathcal{G}_2}{4}(1 + \mathcal{A}_3^2)$ etc. It will soon become clearer why we want to express the potential (3.48) in this way.

However there is one nagging issue that might be bothering the reader, namely, how do we know that the potential (3.48) or equivalently (3.47) only has a linear term? To answer this question convincingly, we go to the next section where we provide a generic derivation of the linear term.

3.1.3 Generic argument for confinement

In the above subsection we argued for the linear potential taking all \mathcal{A}_n for $n \geq 1$ to be small. This is consistent with the *supergravity* limit of our background because in this limit we expect $g_s \rightarrow 0$ and $g_s N_f \rightarrow 0$ with $g_s N \rightarrow \infty$. For these choices of \mathcal{A}_n , (3.39) will imply $z_{\max} < 1$ because we expect \tilde{u}_{\max} to take the highest value in Region 3. Under such a situation, condition like (3.40) will be fully under control, and an analysis of the Wilson loop above reproduces the required linear potential at large d .

However a little thought will tell us that the above derivation cannot be the complete story. What if u_{\max} , in appropriate units, is of order $(1 - \epsilon)$ where $\epsilon \rightarrow 0$? In that case its inverse z_{\max} is of order 1, so both u_{\max} and z_{\max} can no longer be good expansion parameters. We may also consider simultaneously the case where g_s is no longer small so that \mathcal{A}_n for $n \geq 1$ are not small either. Such choices will take us away from the supergravity limit that we have been following. In this limit, we want to ask whether we can still show linear confinement of quarks. Or more generically we want to study confinement for a choice of u_{\max} that saturates the inequality (3.28) but does not presuppose any limiting behavior of u_{\max} , \mathcal{A}_n or \mathcal{G}_n .

In the following therefore we will analyze the integrals (3.25) and (3.33) in the limit u_{\max} is close to its upper bound set by (3.28) (see also [36]). In particular if \mathbf{u}_{\max} is the upperbound of u_{\max} , then it is found by solving

$$\frac{1}{2}(m+1)\mathcal{A}_{m+3}\mathbf{u}_{\max}^{m+3} = 1 \quad (3.49)$$

We observe that both the integrals (3.25) and (3.33) are dominated by $v \sim 1$ behaviour of the integrands. Near $v = 1$ and $u_{\max} \rightarrow \mathbf{u}_{\max}$ the distance d between the quark and the antiquark can be written as:

$$\begin{aligned} d &= 2 \frac{\sqrt{\mathcal{G}_m \mathbf{u}_{\max}^m} \mathbf{u}_{\max}}{\mathcal{A}_n \mathbf{u}_{\max}^n} \int_0^1 \frac{dv}{\sqrt{\mathbf{A}(1-v) + \mathbf{B}(1-v)^2}} \\ &= -2 \frac{\sqrt{\mathcal{G}_m \mathbf{u}_{\max}^m} \mathbf{u}_{\max}}{\mathcal{A}_n \mathbf{u}_{\max}^n} \left[\frac{\log \mathbf{A} - \log \left(2\sqrt{\mathbf{B}(\mathbf{A} + \mathbf{B})} + 2\mathbf{B} + \mathbf{A} \right)}{\sqrt{\mathbf{B}}} \right] \end{aligned} \quad (3.50)$$

where note that we have taken the lower limit to 0. This will not change any of our conclusion as we would soon see. On the other hand, the renormalised Nambu-Goto action for the string now becomes:

$$\begin{aligned} S_{\text{NG}}^{\text{ren}} &= \frac{T}{\pi} \frac{\sqrt{\mathcal{G}_m \mathbf{u}_{\max}^m}}{\mathbf{u}_{\max}} \left[\int_0^1 \frac{dv}{\sqrt{\mathbf{A}(1-v) + \mathbf{B}(1-v)^2}} - 1 \right] - \frac{T}{\pi \mathbf{u}_{\max}} + \mathcal{O}(\mathbf{u}_{\max}^2) \\ &= -\frac{T}{\pi} \frac{\sqrt{\mathcal{G}_m \mathbf{u}_{\max}^m}}{\mathbf{u}_{\max}} \left[\frac{\log \mathbf{A} - \log \left(2\sqrt{\mathbf{B}(\mathbf{A} + \mathbf{B})} + 2\mathbf{B} + \mathbf{A} \right)}{\sqrt{\mathbf{B}}} - 1 \right] \\ &\quad - \frac{T}{\pi \mathbf{u}_{\max}} + \mathcal{O}(\mathbf{u}_{\max}^2) \end{aligned} \quad (3.51)$$

where \mathbf{A} and \mathbf{B} are defined as:

$$\begin{aligned} \mathbf{A} &= 4 - 2 \frac{n \mathcal{A}_n u_{\max}^n}{\mathcal{A}_m u_{\max}^m} \\ \mathbf{B} &= 8 \frac{n \mathcal{A}_n u_{\max}^n}{\mathcal{A}_m u_{\max}^m} - 3 \left(\frac{n \mathcal{A}_n u_{\max}^n}{\mathcal{A}_m u_{\max}^m} \right)^2 + \frac{(n^2 - n) \mathcal{A}_n u_{\max}^n}{\mathcal{A}_m u_{\max}^m} - 6 \end{aligned} \quad (3.52)$$

Observe that in the integral (3.50) and (3.51) we have to take the limit $u_{\max} \rightarrow \mathbf{u}_{\max}$. So \mathbf{A}, \mathbf{B} should be evaluated in the same limit. Interestingly, comparing (3.52) to (3.49) we see that

$$\lim_{u_{\max} \rightarrow \mathbf{u}_{\max}} \mathbf{A} \rightarrow 0 \quad (3.53)$$

thus vanishes when computed exactly at \mathbf{u}_{\max} . The other quantity \mathbf{B} remains finite at that point and in fact behaves as:

$$\mathbf{B} = \frac{n^2 \mathcal{A}_n \mathbf{u}_{\max}^n}{\mathcal{A}_m \mathbf{u}_{\max}^m} - 4 > 0 \quad (3.54)$$

Our above computation would mean that the distance d between the quark and the antiquark, and the Nambu-Goto action will have the following dominant behavior:

$$\begin{aligned} d &= \lim_{\epsilon \rightarrow 0} \frac{2\sqrt{\mathcal{G}_m \mathbf{u}_{\max}^m} \mathbf{u}_{\max}}{\mathcal{A}_n \mathbf{u}_{\max}^n} \frac{\log \epsilon}{\sqrt{\mathbf{B}}} \\ S_{\text{NG}}^{\text{ren}} &= \lim_{\epsilon \rightarrow 0} \frac{T}{\pi} \frac{\sqrt{\mathcal{G}_m \mathbf{u}_{\max}^m}}{\mathbf{u}_{\max}} \frac{\log \epsilon}{\sqrt{\mathbf{B}}} \end{aligned} \quad (3.55)$$

which means both of them have identical logarithmic divergences. Thus the finite quantity is the *ratio* between the two terms in (3.55). This gives us:

$$\frac{S_{\text{NG}}^{\text{ren}}}{d} = \frac{T}{\pi} \frac{\mathcal{A}_n \mathbf{u}_{\text{max}}^n}{\mathbf{u}_{\text{max}}^2} = T \times \text{constant} \quad (3.56)$$

Now using the identity (3.4) and the above relation (3.56) we get our final result:

$$V_{Q\bar{Q}} = \left(\frac{\mathcal{A}_n \mathbf{u}_{\text{max}}^n}{\pi \mathbf{u}_{\text{max}}^2} \right) d \quad (3.57)$$

which is the required linear potential between the quark and the antiquark. Observe that the above potential has exactly the same form as (3.48), justifying the fact that $\mathcal{O}(d^2)$ terms are not generated for this case.

Before we end this section one comment is in order. The result for linear confinement only depends on the existence of \mathbf{u}_{max} which comes from the constraint equation (3.49). We have constructed the background such that \mathbf{u}_{max} lies in Region 3, although a more generic case is essentially doable albeit technically challenging without necessarily revealing new physics. For example when $\mathbf{u}_{\text{max}}^{-1}$ is equal to the size of the blown up S^3 at the IR will require us to consider a Wilson loop that goes all the way to Region 1. The analysis remains somewhat identical to what we did before except that in Regions 2 and 1 we have to additionally consider B_{NS} fields of the form $u^{\epsilon(\alpha)}$ and $\log u$ respectively. Of course both the metric and the dilaton will also have non-trivial u -dependences in these regions. One good thing however is that the Wilson loop computation have no UV or IR divergences whatsoever despite the fact that now the analysis is technically more challenging. Our expectation would be to get similar linear behavior as (3.57) here too. We will however leave a more detailed exposition of this for future works.

3.2 Computing the Nambu-Goto Action: Non-Zero Temperature

After studying the zero temperature behavior it is now time to discuss the case when we switch on a non-zero temperature i.e make $g(u) < 1$ or equivalently the inverse horizon radius, u_h finite in (3.8), where

$$g(u) = 1 - \frac{u^4}{u_h^4} \quad (3.58)$$

Choosing the same quark world line (3.7) and the string embedding (3.10) with the same boundary condition (3.11) but now in Euclidean space with compact time direction, the string action at finite temperature can be written as

$$S_{\text{NG}} = \frac{T}{2\pi} \int_{-\frac{d}{2}}^{+\frac{d}{2}} \frac{dx}{u^2} \sqrt{g(u) \left(\mathcal{A}_n u^n \right)^2 + \left[\mathcal{G}_m u^m - \frac{2g_s^2 \tilde{\mathcal{D}}_{n+m_o} \tilde{\mathcal{D}}_{l+m_o} \mathcal{A}_k u^{4+n+l+k+2m_o}}{u_h^4} \right] \left(\frac{\partial u}{\partial x} \right)^2} \quad (3.59)$$

where $\mathcal{G}_m u^m$ is defined in (3.19) and the correction to $\mathcal{G}_m u^m$ is suppressed by g_s^2 as well as u^4/u_h^4 because the background dilaton and non-zero temperature induces a slightly different world-sheet metric than what one would have naively taken. To avoid clutter, one can further redefine these corrections as:

$$\mathcal{G}_m u^m - \frac{2g_s^2 \tilde{\mathcal{D}}_{n+m_o} \tilde{\mathcal{D}}_{l+m_o} \mathcal{A}_k u^{4+n+l+k+2m_o}}{u_h^4} \equiv \tilde{\mathcal{D}}_l u^l \quad (3.60)$$

Minimizing this action gives the equation of motion for $u(x)$ and using the exact same procedure as for zero temperature, the corresponding equation for the distance between the quarks can be written as:

$$d = 2u_{\max} \int_0^1 dv \left\{ v^2 \sqrt{\tilde{\mathcal{D}}_m u_{\max}^m v^m} \frac{\sqrt{1 - \frac{u_{\max}^4}{u_h^4}} \mathcal{A}_n u_{\max}^n}{\left(1 - \frac{v^4 u_{\max}^4}{u_h^4}\right) (\mathcal{A}_m u_{\max}^m v^m)^2} \right. \\ \left. \left[1 - v^4 \frac{\left(1 - \frac{u_{\max}^4}{u_h^4}\right)}{\left(1 - \frac{v^4 u_{\max}^4}{u_h^4}\right)} \left(\frac{\mathcal{A}_n u_{\max}^n}{\mathcal{A}_m u_{\max}^m v^m} \right)^2 \right]^{-1/2} \right\} \quad (3.61)$$

Once we have d , the renormalized Nambu-Goto action can also be written following similar procedure. The result is

$$S_{\text{NG}}^{\text{ren}} = \frac{T}{\pi} \frac{1}{u_{\max}} \left\{ -\hat{\mathcal{D}}_0 + \sum_{l=2} \frac{\hat{\mathcal{D}}_l}{l-1} - \int_0^1 \frac{dv}{v^2} \sqrt{\tilde{\mathcal{D}}_m u_{\max}^m v^m} + \mathcal{O}(g_s^2) \right. \\ \left. + \int_0^1 \frac{dv}{v^2} \sqrt{\tilde{\mathcal{D}}_m u_{\max}^m v^m} \left[1 - v^4 \frac{\left(1 - \frac{u_{\max}^4}{u_h^4}\right)}{\left(1 - \frac{v^4 u_{\max}^4}{u_h^4}\right)} \left(\frac{\mathcal{A}_n u_{\max}^n}{\mathcal{A}_m u_{\max}^m v^m} \right)^2 \right]^{-1/2} + \mathcal{O}(\epsilon_o) \right\} \quad (3.62)$$

which is somewhat similar in form with (3.33), which we reproduce in the limit $u_h \rightarrow \infty$. Also as in (3.33), we have defined $\sqrt{\tilde{\mathcal{D}}_m u_{\max}^m v^m} \equiv \hat{\mathcal{D}}_l v^l$.

Now just like the zero temperature case, requiring that d be real, sets an upper bound to u_{\max} , that we denote again by \mathbf{u}_{\max} , and is found by solving the following equation:

$$\frac{1}{2}(m+1) \mathcal{A}_{m+3} \mathbf{u}_{\max}^{m+3} + \frac{1}{j!} \prod_{k=0}^{j-1} \left(k - \frac{1}{2} \right) \left(\frac{\mathbf{u}_{\max}^4}{u_h^4} \right)^j \left[\mathcal{A}_l \mathbf{u}_{\max}^l \left(\frac{l}{2} + 2j - 1 \right) \right] = 1 \quad (3.63)$$

Once we fix u_h and the coefficients of the warp factor \mathcal{A}_n , \mathbf{u}_{\max} will be known. We will assume that \mathbf{u}_{\max} lies in Region 3.

Rest of the analysis is almost similar to the zero temperature case, although the final conclusions would be quite different. To proceed further, let us define certain

new variables in the following way:

$$\begin{aligned}
\tilde{\mathcal{A}}_l &= \sum_m \frac{\mathcal{A}_m}{u_h^{l-m}} \frac{1}{\left(\frac{l-m}{4}\right)!} \prod_{k=0}^{\frac{l-m}{4}-1} \left(k - \frac{1}{2}\right), & l-m \geq 4 \\
&= 0 & l-m < 4 \\
&= \mathcal{A}_l & l-m = 0
\end{aligned} \tag{3.64}$$

As before, we observe that for $u_{\max} \rightarrow \mathbf{u}_{\max}$, both the integrals (3.61),(3.62) are dominated by the behaviour of the integrand near $v \sim 1$, where we can write

$$\begin{aligned}
d &= 2 \frac{\sqrt{\tilde{\mathcal{D}}_m \mathbf{u}_{\max}^m \mathbf{u}_{\max}}}{\sqrt{1 - \frac{\mathbf{u}_{\max}^4}{u_h^4} \mathcal{A}_n \mathbf{u}_{\max}^n}} \int_0^1 \frac{dv}{\sqrt{\tilde{\mathbf{A}}(1-v) + \tilde{\mathbf{B}}(1-v)^2}} \\
&= -2 \frac{\sqrt{\tilde{\mathcal{D}}_m \mathbf{u}_{\max}^m \mathbf{u}_{\max}}}{\sqrt{1 - \frac{\mathbf{u}_{\max}^4}{u_h^4} \mathcal{A}_n \mathbf{u}_{\max}^n}} \left[\frac{\log \tilde{\mathbf{A}} - \log \left(2\sqrt{\tilde{\mathbf{B}}(\tilde{\mathbf{A}} + \tilde{\mathbf{B}})} + 2\tilde{\mathbf{B}} + \tilde{\mathbf{A}} \right)}{\sqrt{\tilde{\mathbf{B}}}} \right]
\end{aligned} \tag{3.65}$$

where taking the lower limit of the integral to 0 again do not change any of our conclusion. On the other hand, the renormalised Nambu-Goto action for the string now becomes:

$$\begin{aligned}
S_{\text{NG}}^{\text{ren}} &= \frac{T}{\pi} \frac{\sqrt{\tilde{\mathcal{D}}_m \mathbf{u}_{\max}^m}}{\mathbf{u}_{\max}} \left[\int_0^1 \frac{dv}{\sqrt{\tilde{\mathbf{A}}(1-v) + \tilde{\mathbf{B}}(1-v)^2}} - 1 \right] - \frac{T}{\pi \mathbf{u}_{\max}} + \mathcal{O}(\mathbf{u}_{\max}^2) \\
&= -\frac{T}{\pi} \frac{\sqrt{\tilde{\mathcal{D}}_m \mathbf{u}_{\max}^m}}{\mathbf{u}_{\max}} \left[\frac{\log \tilde{\mathbf{A}} - \log \left(2\sqrt{\tilde{\mathbf{B}}(\tilde{\mathbf{A}} + \tilde{\mathbf{B}})} + 2\tilde{\mathbf{B}} + \tilde{\mathbf{A}} \right)}{\sqrt{\tilde{\mathbf{B}}}} - 1 \right] \\
&\quad - \frac{T}{\pi \mathbf{u}_{\max}} + \mathcal{O}(\mathbf{u}_{\max}^2)
\end{aligned} \tag{3.66}$$

where $\tilde{\mathbf{A}}$ and $\tilde{\mathbf{B}}$ are defined exactly as in (3.52) but with \mathcal{A}_n replaced by $\tilde{\mathcal{A}}_n$ given by (3.64) above. It is also clear that:

$$\lim_{u_{\max} \rightarrow \mathbf{u}_{\max}} \tilde{\mathbf{A}} \rightarrow 0 \tag{3.67}$$

and so both (3.65) as well as (3.66) have identical logarithmic divergences. This would imply that the finite quantity is the ratio between (3.66) and (3.65):

$$\frac{S_{\text{NG}}^{\text{ren}}}{d} = \frac{T}{\pi} \left(1 - \frac{\mathbf{u}_{\max}^4}{u_h^4} \right)^{\frac{1}{2}} \frac{\mathcal{A}_n \mathbf{u}_{\max}^n}{\mathbf{u}_{\max}^2} \tag{3.68}$$

Now using the identity (3.6) and the above relation (3.56) we get our final result:

$$V_{Q\bar{Q}} = \sqrt{1 - \frac{\mathbf{u}_{\max}^4}{u_h^4}} \left(\frac{\mathcal{A}_n \mathbf{u}_{\max}^n}{\pi \mathbf{u}_{\max}^2} \right) d \tag{3.69}$$

3.2.1 Analysis of the melting temperature

To determine the behavior of the potential $V_{Q\bar{Q}}$ as the temperature is raised or decreased (or u_h is decreased or increased respectively) we have to carefully analyse the behavior of \mathbf{u}_{\max} as a function of u_h . Comparing this with (3.63) and fixed \mathcal{A}_n we observe that

$$\frac{\delta \mathbf{u}_{\max}}{\delta u_h} = \frac{\frac{1}{j!} \prod (k - \frac{1}{2}) \frac{\mathbf{u}_{\max}^{4j}}{u_h^{4j+1}} \mathcal{A}_l u^l (\frac{l}{2} + 2j - 1)}{\frac{1}{2} m(m+1) \mathcal{A}_m u^m + \frac{1}{j!} \prod (k - \frac{1}{2}) \frac{\mathbf{u}_{\max}^{4j-1}}{u_h^{4j}} \mathcal{A}_l u^l (4j + l) (\frac{l}{2} + 2j - 1)} \quad (3.70)$$

where the repeated indices are all summed over and the product runs from $k = 0$ to $k = j - 1$. Observe that the numerator of (3.70) is always negative, and for large u_h the denominator will be positive (because we are taking all $\mathcal{A}_n > 0$). This means

$$\frac{\delta \mathbf{u}_{\max}}{\delta u_h} < 0$$

and therefore as u_h is decreased (i.e the temperature is increased), \mathbf{u}_{\max} increases making the ratio $\frac{u_{\max}^4}{u_h^4}$ to increase. This in turn would imply that the slope of the potential $V_{Q\bar{Q}}$ decreases. Therefore there would be a temperature where the slope would be minimum and the system would show the property of *melting*.

To start off let us consider (3.63) for a simple case where we keep u_{\max} only to quartic order²³. This means:

$$\frac{1}{2} \mathcal{A}_3 u_{\max}^3 + \left(\mathcal{A}_4 - \frac{1}{2u_h^4} \right) u_{\max}^4 = 1 \quad (3.71)$$

This is a quartic equation and one can easily solve it for u_{\max} . To make the analysis a little more simpler, let us also assume $\mathcal{A}_3 = 0$. Such a choice will immediately give us the following potential between the quark and the antiquark:

$$V_{Q\bar{Q}} = \left[\left(1 + \frac{\mathcal{A}_2}{\pi} \right) + \frac{1}{\pi} \sqrt{\mathcal{A}_4 - \frac{1}{2u_h^4}} \right] d \quad (3.72)$$

which tells us that u_h has to be bounded by

$$u_h > \frac{0.84}{\mathcal{A}_4^{1/4}}$$

for (3.72) to make sense, and the slope of the potential would decrease as u_h approaches this value. On the other hand u_{\max} increases as u_h is lowered and for

$$u_h = \frac{1.1067}{\mathcal{A}_4^{1/4}} \quad (3.73)$$

²³This is a subtle issue because we are *truncating* the series (3.63) and especially u_h to only this order to have an analytic control on our calculations. A more generic analysis can be done numerically, which we present in the next section.

we expect the potential to have a minimum slope where the onset of *melting* should appear. A temperature greater than this is physically not possible because the string would break. Also note if we kept $\mathcal{A}_0 \neq 1$, we would have $(\mathcal{A}_0/\mathcal{A}_4)^{1/4}$ in (3.73).

The above conclusion is certainly interesting, but may be a little naive because there is no strong reason to terminate the constraint (3.63) to \mathcal{A}_4 because (3.64) would tell us that higher powers of u_{\max} will have all the lower \mathcal{A}_n 's as coefficients. This would make the subsequent analysis complicated, and we have to resort to numerical methods.

On the other hand the above analysis does shed some light on the situation where the ratio $\frac{u_{\max}^4}{u_h^4} > 1$. It is clear from our above calculation what happens when u_h becomes too small: since by lowering u_h there is an increase in \mathbf{u}_{\max} , we are always bounded by the constraint:

$$\mathbf{u}_{\max} \leq u_h \tag{3.74}$$

where the equality would lead to (3.73). Therefore for (3.72) and (3.74) to make sense, the string connecting quark and the antiquark should *break* when \mathbf{u}_{\max} starts exceeding u_h as mentioned above. This is the point where total melting happens, and the linear potential goes from the minimum slope σ , where

$$\sigma \equiv \frac{V_{Q\bar{Q}}}{d} = 1 + 0.32 \mathcal{A}_2 \tag{3.75}$$

to zero as soon as the temperature is increased, or alternatively u_h is decreased, beyond (3.73). In fact beyond certain temperature, constraint equation like (3.63) is no longer valid, and we are only left with the Coulombic term that eventually dies off at large distances.

3.3 Numerical analysis

Most of the calculations that we did in the previous sections have been analytic. Under some approximations we could see certain important properties of quark-antiquark potentials at zero and non-zero temperatures. However as mentioned in the footnote earlier, truncating the series (3.63) as (3.71) may not capture the full story although the above toy example does give us a way to compute the melting temperature where the slope of the potential hits a minima (3.75). Our main conclusion of the previous section is that there exists a set of warp factors \mathcal{A}_n for which the equality $\mathbf{u}_{\max} = u_h$ is valid. That means out of a large sets of possible backgrounds (classified by the choices of warp factors satisfying EOMs) this equality would select a particular subset of backgrounds that allow deconfinement and quarkonium meltings at the temperatures (3.73) for a subset of \mathcal{A}_4 in this approximation. What happens if we choose an arbitrary set of warp factors that do not lie in this subset? In this section we will perform a numerical analysis to study the behavior of the quark-antiquark potentials for this case at all temperatures.

For this particular choice of coefficients of the warp factor we can numerically compute the interquark distance d in (3.25), (3.61) and the NG action $S_{\text{NG}}^{\text{ren}}$ (3.29),(3.62), for various values of u_{max} and using this, plot $V_{Q\bar{Q}}$ as a function of d . The analytic behavior of d and $V_{Q\bar{Q}}$ discussed in the previous sections for u_{max} very large and small will turn out to be consistent with our numerical analysis although the property of melting will not be visible now. For simplicity we will choose the following values for the coefficients of the warp factor:

$$\mathcal{A}_0 = 1, \quad \mathcal{G}_0 = 1, \quad \mathcal{A}_2 = \mathcal{A}_4 = \mathcal{G}_2 = \mathcal{G}_4 = 0.24 \quad (3.76)$$

with $g_s \sim 0.02$ and $N_f = 24$. This is indeed a reasonable choice, and hopefully satisfies EOMs despite being outside the required subset, because as we saw from F-theory, all corrections to warp factor due to running of the τ field comes as $\mathcal{O}(g_s^2 N_f^2)$. Figure 7 shows how the inter-quark distance d varies with u_{max} . For $T = 0$, from the

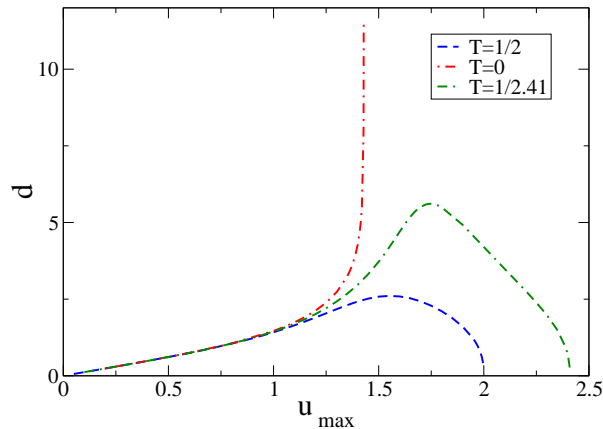


Figure 7: Inter-quark distance d as a function of u_{max} evaluated for our choice of warp factor given earlier. The red curve is the zero temperature limit. Here $T \equiv 1/u_h \equiv r_h$ henceforth.

figure we see that there exists an upper bound u_{max} near which $d \rightarrow \infty$. A similar analysis also gives as $u_{\text{max}} \rightarrow u_{\text{max}}$, $V_{Q\bar{Q}} \rightarrow \infty$. By increasing u_{max} near u_{max} , we can get *all* the values of d and $V_{Q\bar{Q}}$ and using this we can plot $V_{Q\bar{Q}}$ as a function of d as shown in Figure 8. Note that for large d , the potential grows exactly linear with distance indicating linear confinement. This is consistent with our earlier analytical calculations. Additionally for small distances, the potential behaves like a Coulomb potential as also predicted by our analysis. On the other hand for $T \neq 0$, again for the choice of our warp factors (3.76), from Figure 7 we observe that for every $T \neq 0$ curve, there exists a maximum value of d , say d_{max} and therefore for every value of d , there are two distinct values for u_{max} . Such a behavior has also been observed in [20]

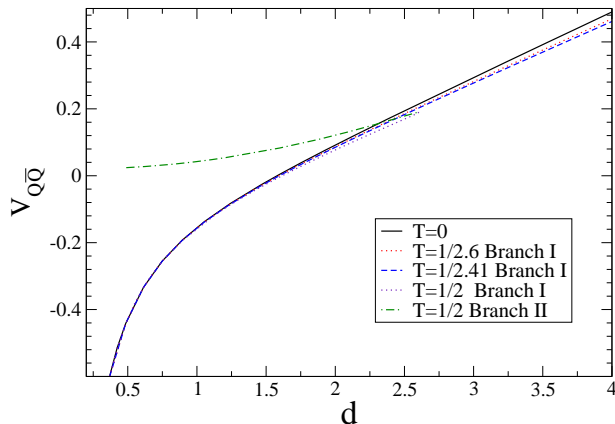


Figure 8: Quarkonium potential as a function of inter quark distance d at various temperatures. Note the linear and the Coulombic behaviors at large and small distances respectively.

for the AdS case and in [19, 21] for the pure Klebanov-Strassler case. This means for a particular choice of d and boundary condition $u(\pm d/2) = 0$, there are two U -shaped strings with two values for u_{\max} , namely $u_{\max,1}$ and $u_{\max,2}$ with $u_{\max,2} > u_{\max,1}$. As $u_{\max,2} > u_{\max,1}$, the U -shaped string with $u_{\max,2}$ has higher energy than the one with $u_{\max,1}$. We have denoted the U -shaped string with $u_{\max,1}$ by branch I and the one with $u_{\max,2}$ by branch II in Figure 8. It is clear from the plot that branch I has lower energy than branch II. Thus at small d , the potential for branch I behaves as Coulomb potential and by comparing this to the zero temperature Coulomb behavior, we see that the $T \neq 0$ Coulomb potential is suppressed.

Now note that as we lower the temperature, the value for d_{\max} increases. Therefore in the limit $T \rightarrow 0$, $d_{\max} \rightarrow \infty$, which is perfectly consistent with our zero temperature curve in Figure 7. This implies as $T \rightarrow 0$, the curves in Figure 7 converge with the zero temperature curve, which in turn blows up at \mathbf{u}_{\max} . Such a behavior is not inconsistent with the high temperature case because we can view the $T = 0$ curve to go straight up and never come down, resulting in a single solution for the U -shaped string for every d . The high temperature curves go upto some d_{\max} and then come down. For large $d < d_{\max}$, we have linear potential for branch I – which is suppressed compared to the zero temperature curve as shown in Figure 8. As the temperature is increased more is the suppression and smaller is the value for d_{\max} .

In Figure 8 with our choice of the warp factor coefficients the slopes of linear potentials and the resulting suppressions are not very significant. For a better view of the suppressions, we present a blown up version of Figure 8 in Figure 9.

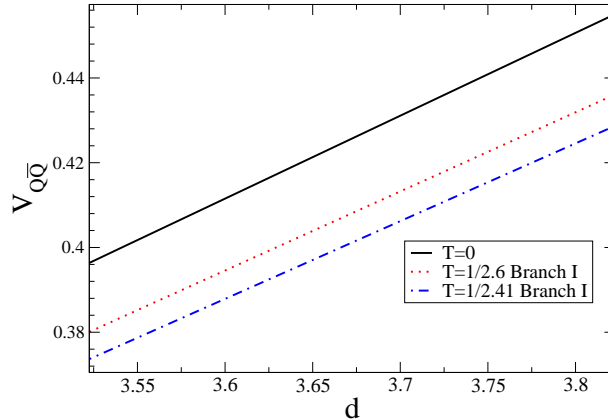


Figure 9: Suppressions at non zero temperatures of the linear potential magnified by choosing a slightly different values of the coefficients of the warp factor given earlier. In this figure one can clearly see how with high temperatures the quark-antiquark potentials melt.

For $d > d_{\max}$, there is no real solution to the differential equation for $u(x)$ with boundary condition $u(\pm d/2) = 0$ and thus there is no U -shaped string between the quarks. Thus for $d > d_{\max}$, the string breaks and we have deconfined quarks. Also as d_{\max} decreases with increasing temperature, at high temperatures the quarks get screened at shorter distances – which is consistent with heavy quarkonium suppression in thermal QCD.

Our numerical analysis and the plots should be instructive for a generic choice of the coefficients of the warp factor where we again may not see the melting temperature. To study the generic case, first consider the zero temperature limit. Note that the existence of real positive \mathbf{u}_{\max} is guaranteed if all $\tilde{\mathcal{A}}_n$ in (3.64) are positive. However this may not be true if the original warp factor coefficients \mathcal{A}_n are a *finite* set²⁴. This is because for a finite set of \mathcal{A}_n 's, there will be some $\tilde{\mathcal{A}}_n$'s which are negative and the equation

$$\frac{m+1}{2} \tilde{\mathcal{A}}_{m+3} \mathbf{u}_{\max}^{m+3} = 1 \quad (3.77)$$

may not have any real positive solutions. This would imply the existence of d_{\max} and consequently two branches of solution. For large $d < d_{\max}$, we will have linear potentials with suppressions at higher temperatures with lower values of d_{\max} .

On the other hand, at zero temperature if all $\mathcal{A}_n > 0$, there is always a positive real \mathbf{u}_{\max} and we will have linear potential at large distances. If some \mathcal{A}_n 's are

²⁴As should be obvious from (3.64), a finite set of \mathcal{A}_n still implies an infinite set of $\tilde{\mathcal{A}}_n$.

negative, we could have no real positive solution \mathbf{u}_{\max} which means $0 \leq u_{\max} \leq \infty$ as there is no black hole horizon. In this case the behavior of d will be dominated by $d \sim u_{\max}$ and that of $V_{Q\bar{Q}}$ will be dominated by $V_{Q\bar{Q}} \sim 1/u_{\max}$ which means $V_{Q\bar{Q}} \sim 1/d$ – and we will have the Coulomb potential for all d .

Our above numerical analysis certainly illustrates the decrease in the slope of the linear potential as the temperature is increased but *does not* show us the melting temperature. What would happen if we restrict our warp factor choice to the required subset of \mathcal{A}_n ? In this case all the high temperature curves will grow linearly and will not come back, and at a certain temperature the slope of the curve will drop to zero. This will be the melting temperature. In this paper we will not pursue this anymore, and more details will be presented elsewhere.

4. Conclusions and Discussions

In this paper we have tried to achieve two goals: First is to find the dual to large N gauge theory that resembles large N QCD i.e. at far IR the theory confines and at far UV the theory shows a conformal behavior. We then extend this to high temperatures. Second, is to compute the heavy quarkonium potential in this theory both at zero and non-zero temperatures. We have shown that, under some rather generic conditions, zero temperature linear confinement for heavy quarkonium states can be demonstrated. At high temperature, the expected deconfinement and quarkonium melting follow from our analysis.

There are however still a few loose ends that need to be tightened to complete the full story. The first one is the issue of supersymmetry. Although we have shown that all the unnecessary tachyons can be removed from our picture, this still doesn't imply low energy supersymmetry in our model (at zero temperature). Having *no* supersymmetry should be viewed as desirable because we don't expect low energy susy in real world! However susy breaking in our model may trigger corrections in the potential that need to be worked out. We expect these corrections to change the coefficient of the linear term *without* generating an $\mathcal{O}(d^2)$ term. These corrections should be higher orders in $g_s N_f$, so will not change any of our conclusions presented here. This is because the linear potential arises from the limit where the Nambu-Goto action and the distance d exhibit identical logarithmic divergences. This behavior should remain the same whether or not we have low energy susy in our model or not. Thus the linear confinement argument is particularly robust for our case. On the other hand the Coulombic behavior is model independent, so the coefficient of the Coulombic term should remain unchanged whether we take susy or non-susy models (see for example the model of [36]). One may choose other embeddings of seven-branes, like [22] or the model studied in [18], to study the quarkonium potentials at zero and non-zero temperatures. But such choices of embeddings will not change our main conclusions.

The second one is the issue of Higgsing that breaks the gauge group from $SU(N+M) \times SU(N+M)$ to $SU(N+M) \times SU(N)$ in the gauge theory side. As mentioned in sec. 2.3, the story in the dual gravity side is somewhat clearer. What one needs is to analyse the gauge theory operators carefully that will allow the above mentioned Higgsing. We leave this for future work.

The third one is to find the precise set of warp factors \mathcal{A}_n that satisfy EOMs and allow us to get the melting temperature for the heavy quarkonium states. In the previous section we gave a numerical analysis with an arbitrary truncated set of warp factors that shows the decrease in the slope of the linear potential with increasing temperatures. Our numerical analysis certainly shows the possibility of melting, but doesn't tell us the melting temperature. On the other hand our analytic way of getting the melting temperature is not very generic. So it would be interesting to find the full set of warp factors to complete the story²⁵.

Finally, we haven't actually computed the exact gauge fluxes on the seven and five-branes that would cancel the tachyons in this model. Following the works of [26] this may not look like a difficult task to do, at least for the flat background. What makes it non-trivial here is that all the branes are embedded in a *curved* background. Quantisation of strings in a curved background is highly non-trivial, so it'll be rather challenging to work this out in full details. Nevertheless, if we restrict everything to Region 3 and away from the brane-antibrane systems, these subtleties will not affect our results in any significant way. Happily this is the regime where most of our calculations have been performed in this paper.

Note: As this draft was being written, we became aware of the work of Gaillard *et al* [37] which has some overlap with this paper. See also the earlier work [38].

Acknowledgements

It's our pleasure to thank Peter Ouyang for many helpful discussions, and comments on the preliminary version of our draft. We would also like to thank Dongsu Bak, Niky Kamran and Omid Saremi for helpful comments. M. M would like to thank the organisers of *String 2010* for comments on the poster demonstration of our work. He would also like to thank Chris Herzog, Dario Martelli, Jorge Noronha and Ashoke Sen for helpful comments. This work is supported in part by the Natural Sciences and Engineering Research Council of Canada, and in part by McGill University.

²⁵Note that in the series of papers [31, 34, 32] similar screening like what we have in (3.69) is also observed using completely different techniques than ours. Our prediction then would be that the square-root suppression that we see in (3.69) at high temperatures is *universal*. Of course it would be interesting to figure out the Coulomb screening at high temperature also.

A. Complete analysis of a background configuration

In this appendix we will, for illustration, compute the background that appears from the backreactions of the seven branes without any three-form fluxes but with five-form fluxes. These five-form fluxes are the remnant of the three-branes. So in the gauge-theory side we will have a system of N D3 branes and N_f seven branes. The excitations of these D3/D7 branes are described by a gauge theory with $SU(N) \times SU(N)$ color symmetry and $SU(N_f) \times SU(N_f)$ flavor symmetry. Holography dictates that the near horizon geometry sourced by these D3/D7 branes is dual to the gauge theory (decoupled from gravity) which arises from the brane excitations. Of course there are two ways to get the gravity dual picture from the brane configuration. We could first obtain the geometry sourced by the D3/D7 system and then take the near horizon limit of it. Or first compute the near horizon geometry of the D3 branes, then place seven-branes in that geometry and finally compute the backreaction. Both this approaches are identical in the limit where the stack of seven-branes are separated from the stack of D3-branes. Therefore for technical simplicity, we will adopt the latter approach. We will also put the configuration in a conifold setting to mimic what we did in [13].

The near horizon geometry of the stack of D3 branes placed at the tip of a conifold is $AdS_5 \times T^{1,1}$. We embed the seven-branes in this background with the world-volume filling up four Minkowski directions plus a four-cycle in $T^{1,1}$, and compute the backreaction. The supergravity action describing the geometry in Einstein frame is

$$S_{\text{SUGRA}} = \frac{1}{2\kappa_{10}^2} \int d^{10}x \sqrt{G} \left(R + \frac{\partial_\mu \bar{\tau} \partial^\mu \tau}{2|\text{Im}\tau|^2} - \frac{1}{2} |\tilde{F}_5|^2 \right) + S_{\text{D7}}^{\text{loc}} + \int_{\Sigma_8} C_4 \wedge R_{(2)} \wedge R_{(2)} \quad (\text{A.1})$$

where τ is the axio-dilaton field, \tilde{F}_5 is the five-form fluxes sourced by the D3 branes, C_4 is the pull-back of the four-form potential, $G = \sqrt{\det G_{\mu\nu}}$ with $G_{\mu\nu}$ being the metric, $R_{(2)}$ is the curvature two-form, and $S_{\text{D7}}^{\text{loc}}$ is the local action for the seven-branes. There are additional Chern-Simons couplings of the seven-brane gauge fields to the background RR forms, but we will ignore them for the time being. They will appear later.

Varying the action with respect to the various fields give rise to the background equations of motion. Using our earlier notations, they are given by (2.27) (without the (p, q) five-brane terms) and (2.28) (again removing the (p, q) five-brane contribution) for the metric and the five-form respectively. Our metric ansatz remains

$$ds^2 = \frac{1}{\sqrt{h}} \left[-g(r) dt^2 + dx^2 + dy^2 + dz^2 \right] + \sqrt{h} \left[g(r)^{-1} g_{rr} dr^2 + g_{mn} dx^m dx^n \right] \quad (\text{A.2})$$

as before, with $g(r)$ being the Black-Hole factor and h being the warp factor that depends on all the internal coordinates $(r, \theta_i, \phi_i, \psi)$. To zeroth order in $g_s N_f$ we have

our usual relations:

$$h^{[0]} = \frac{L^4}{r^4}, \quad g^{[0]} = 1 - \frac{r_h^4}{r^4}, \quad g_{rr}^{[0]} = 1, \quad g_{mn}^{[0]} dx^m dx^n = ds_{T^{11}}^2 \quad (\text{A.3})$$

But in higher order in $g_s N_f$, both the warp factor and the internal metric get modified because of the back-reactions from the seven-branes. We can write this as:

$$h = h^{[0]} + h^{[1]}, \quad g_{rr} = g_{rr}^{[0]} + g_{rr}^{[1]}, \quad g_{mn} = g_{mn}^{[0]} + g_{mn}^{[1]} \quad (\text{A.4})$$

where the superscripts denote the order of $g_s N_f$.

Using the full F-theory completion of the background as discussed in section 2.3, we know that near any one of the seven-branes, i.e $z \sim z_k$:

$$\tau \sim \log(z - z_k) \quad (\text{A.5})$$

and therefore the internal metric components will typically behave as:

$$g_{rr}^{[1]} = \sum_{i,j} a_{rr,ij}^{[1]} \frac{\log^i(r)}{r^j}, \quad g_{mn}^{[1]} = \sum_{i,j} a_{mn,ij}^{[1]} \frac{\log^i(r)}{r^{j-2}} \quad (\text{A.6})$$

with $a_{mn,ij}^{[1]}$ independent of r but depend on the internal coordinates (ψ, θ_i, ϕ_i) .

Now away from $z \sim z_k$, we can use similar discussion as in sec. 2.3 with axio-dilaton τ behaving exactly as (2.33). In that case the internal components of the metric become:

$$g_{mn}^{[1]} = \sum_{i=0}^{\infty} \frac{a_{mn,i}^{[1]}}{r^{i-2}}, \quad g_{rr}^{[1]} = \sum_{i=0}^{\infty} \frac{a_{rr,i}^{[1]}}{r^i} \quad (\text{A.7})$$

where again $a_{mn,i}^{[1]}$ are independent of r but depend on the internal coordinates.

Now to find the precise expression for h , we use the five-form equation (2.28). Since both the three-forms vanish for our case, and additionally if we embed part of the spin connection in the seven-brane gauge connection with appropriate number of antiseven-branes, we can easily derive the following warp factor equation:

$$\sum_n \frac{\partial}{\partial x^m} \left(g^{mn} g^{00} \sqrt{-\det g_{ab}} \frac{\partial h}{\partial x^n} \right) = \text{sources} \quad (\text{A.8})$$

as before; where (m, n) now run over all the internal six coordinates. The generic solutions of all the above equations would be

$$h = \frac{L^4}{r^4} \left[1 + \sum_{i=1}^{\infty} \frac{a_i(\psi, \theta_j, \phi_j)}{r^i} \right] \quad \text{for large } r$$

$$h = \frac{L^4}{r^4} \left[\sum_{j,k=0} b_{jk}(\psi, \theta_i, \phi_i) \frac{\log^k r}{r^j} \right] \quad \text{for small } r \quad (\text{A.9})$$

which is of course the solutions (2.7) discussed before, and away from the interpolating region, i.e Region 2. In the next appendix we will discuss a way to determine the coefficients a_i and b_{ij} . Note that the above form of the large r warp factor also implies that the effective number of colors is given by:

$$N_{\text{eff}} = N \left(1 + \sum_{i=1} \frac{a_i}{r^i} \right) \quad (\text{A.10})$$

Thus N_{eff} keeps growing with radial coordinate r for all $a_i < 0$ and $N_{\text{eff}} = N$ at the boundary $r = \infty$. Alternatively, with a change of coordinate $u = 1/r$, the metric will take the following form:

$$ds^2 = g_{\mu\nu} dX^\mu dX^\nu = \mathcal{A}_n(\psi, \theta_i, \phi_i) u^{n-2} [-g(u) dt^2 + d\vec{x}^2] + \frac{\mathcal{B}_l(\psi, \theta_i, \phi_i) u^l}{\mathcal{A}_m(\psi, \theta_i, \phi_i) u^{m+2} g(u)} du^2 + \frac{1}{\mathcal{A}_n(\psi, \theta_i, \phi_i) u^{n+2}} ds_{\mathcal{M}_5}^2 \quad (\text{A.11})$$

which is the metric (3.8) and $ds_{\mathcal{M}_5}^2$ is the metric of the deformed $T^{1,1}$. We note as before that the coefficients C_n depend on the coordinates (ψ, θ_i, ϕ_i) , the locations of the seven-branes, and the number of colors and flavors, N and N_f respectively. For all $C_n > 0$, N_{eff} grows with decreasing u with maximum value at the boundary $u = 0$.

B. Solution to Einstein equations

One last thing that needs to be studied is the deviation of the internal metric from the usual Ricci-flat metric. We already hinted this in sec. 2.3, but now we will keep all the angular coordinates and see whether we can find a possible solution. Our aim therefore is to solve (2.27), keeping only the axio-dilaton sources (2.33) and not the seven-branes and antiseven-branes local energy-momentum tensors. A justification for this can be easily provided: we are using the *effective* embeddings (2.8) and (2.37) for branes and antibranes respectively. The axio-dilaton field (2.33) can alternatively be written as:

$$\tau = \sum_n \mathcal{A}_n z^{-n} = \sum_n \mathcal{A}_n r^{-n} e^{in(\phi_1 + \phi_2 - \psi)} \left[\text{cosec} \left(\frac{\theta_1}{2} \right) \text{cosec} \left(\frac{\theta_2}{2} \right) \right]^n \quad (\text{B.1})$$

The above behavior, as discussed earlier, is valid for all r (in Region 3). Therefore τ has a nice Taylor series expansion and the right hand side of (2.27) will also have a smooth Taylor series. As an illustration, consider

$$\frac{\partial \tau}{\partial r} \frac{\partial \bar{\tau}}{\partial r} = \sum_{k,l} \frac{k l \mathcal{A}_k \mathcal{A}_l}{r^{k+l+2}} e^{i(\phi_1 + \phi_2 - \psi)(k-l)} \text{cosec}^{k+l} \left(\frac{\theta_1}{2} \right) \text{cosec}^{k+l} \left(\frac{\theta_2}{2} \right) \tilde{F}_{rr}(\theta_1, \theta_2) \quad (\text{B.2})$$

where $\tilde{F}_{mn}(\theta_1, \theta_2)$ depends on the partial derivative $|\partial_r \tau|^2$. As the source is a Taylor series in r^{-1} , we must have Ricci-tensor \tilde{R}_{rr} to be a Taylor series. This in turn would imply that the *unwarped* metric components should go like:

$$\tilde{g}_{mn} = \sum_{i=0}^{\infty} \frac{a_{mni}}{r^i} \quad (\text{B.3})$$

where $j = i - 2$ or $j = i$ depending on whether we are choosing the radial direction or not (see sec. 2.3 for details). The coefficients $a_{mni} \equiv a_{mni}(\theta, \phi, \psi)$ i.e functions of all the internal coordinates.

Now to explicitly solve for the partial differential equations involving a_{mni} we observe that the right hand side of (2.27) as a function of internal coordinates (ψ, ϕ_i, θ_i) is of the form $e^{i(\phi_1 + \phi_2 - \psi)}$ and $\text{cosec}(\frac{\theta_i}{2})$. So the most general form for a_{mni} should also involve these variables²⁶. Thus we introduce variables:

$$\begin{aligned} \tilde{z}_1 &= \cos\left(\frac{\theta_1}{2}\right) + i \sin\left(\frac{\theta_1}{2}\right) \\ \tilde{z}_2 &= \cos\left(\frac{\theta_2}{2}\right) + i \sin\left(\frac{\theta_2}{2}\right) \end{aligned} \quad (\text{B.4})$$

and using which we make the following ansatz for a_{mni} :

$$a_{mn\alpha} = a_{mn0} + \sum_{k,l,k+l=\alpha} e^{i(\phi_1 + \phi_2 - \psi)(k-l)} \left[\frac{\tilde{a}_{mn}^{ij}}{\tilde{z}_i \tilde{z}_j^*} + \frac{\tilde{a}_{mn}^{ijop}}{\tilde{z}_i \tilde{z}_j^* \tilde{z}_o \tilde{z}_p^*} \dots + \frac{\tilde{a}_{mn}^{i_1 i_2 \dots i_{2n}}}{\tilde{z}_{i_1} \tilde{z}_{i_2}^* \dots \tilde{z}_{i_{2\alpha-1}} \tilde{z}_{i_{2\alpha}}^*} \right] \quad (\text{B.5})$$

where summation over repeated index is assumed. Note that with this ansatz written in terms of coordinate \tilde{z}_i , the differential equations in (2.27) become a set of algebraic equations because $\sec^n(\theta_i)$, $\text{cosec}^n(\theta_i)$ etc. can be written as a linear combinations of \tilde{z}_i . Then it is straight forward to equate coefficients of various powers of \tilde{z}_i and obtain the *constant* coefficients $\tilde{a}_{i_1 i_2 \dots i_{2n}}$. This gives us the precise procedure to obtain the exact solutions for all a_{mni} . In Region 2 we have to be more careful because there are, in addition to the axio-dilaton, other sources. But since all our calculations are restricted to Region 3, we need not worry too much about the non-Ricci flatness of the internal manifold.

References

- [1] A. Bazavov *et al.*, “Equation of state and QCD transition at finite temperature,” Phys. Rev. D **80**, 014504 (2009) [arXiv:0903.4379 [hep-lat]].
- [2] See, for example, C. Gale, “Photon Production in Hot and Dense Strongly Interacting Matter,” arXiv:0904.2184 [hep-ph], and references therein.

²⁶We thank Niky Kamran for helpful comments.

- [3] See, for example, M. Gyulassy, I. Vitev, X. N. Wang and B. W. Zhang, “Jet quenching and radiative energy loss in dense nuclear matter,” arXiv:nucl-th/0302077, and references therein.
- [4] T. Matsui and H. Satz, “J/psi Suppression by Quark-Gluon Plasma Formation,” Phys. Lett. B **178**, 416 (1986).
- [5] M. Gyulassy and L. McLerran, “New forms of QCD matter discovered at RHIC,” Nucl. Phys. A **750**, 30 (2005) [arXiv:nucl-th/0405013].
- [6] P. Braun-Munzinger, J. Stachel, “(Non)thermal aspects of charmonium production and a new look at J/psi suppression,” Phys. Lett. B **490**, 196 (2000) [arXiv:nucl-th/0007059]; M. I. Gorenstein, A. P. Kostyuk, H. Stoecker and W. Greiner, “Statistical coalescence model with exact charm conservation,” Phys. Lett. B **509**, 277 (2001) [arXiv:hep-ph/0010148]; L. Grandchamp and R. Rapp, “Thermal versus direct J/psi production in ultrarelativistic heavy-ion collisions,” Phys. Lett. B **523**, 60 (2001) [arXiv:hep-ph/0103124]; R. L. Thews and M. L. Mangano, “Momentum spectra of charmonium produced in a quark-gluon plasma,” Phys. Rev. C **73**, 014904 (2006) [arXiv:nucl-th/0505055].
- [7] A. Mocsy, “Quarkonium Spectral Functions,” Nucl. Phys. A **830**, 411C (2009) [arXiv:0908.0746 [hep-ph]].
- [8] O. Kaczmarek, F. Karsch, F. Zantow and P. Petreczky, “Static quark anti-quark free energy and the running coupling at finite temperature,” Phys. Rev. D **70**, 074505 (2004) [Erratum-ibid. D **72**, 059903 (2005)] [arXiv:hep-lat/0406036]; K. Petrov, “Singlet free energies and renormalized Polyakov loop in full QCD,” [RBC-Bielefeld Collaboration], PoS LAT2006, 144 (2006) [arXiv:hep-lat/0610041].
- [9] J. M. Maldacena, “The large N limit of superconformal field theories and supergravity,” Adv. Theor. Math. Phys. **2**, 231 (1998) [Int. J. Theor. Phys. **38**, 1113 (1999)] [arXiv:hep-th/9711200].
- E. Witten, “Anti-de Sitter space, thermal phase transition, and confinement in gauge theories,” Adv. Theor. Math. Phys. **2**, 505 (1998) [arXiv:hep-th/9803131].
- [10] E. Witten, “Anti-de Sitter space and holography,” Adv. Theor. Math. Phys. **2**, 253 (1998) [arXiv:hep-th/9802150].
- S. S. Gubser, I. R. Klebanov and A. M. Polyakov, “Gauge theory correlators from non-critical string theory,” Phys. Lett. B **428**, 105 (1998) [arXiv:hep-th/9802109].
- [11] G. Policastro, D. T. Son and A. O. Starinets, “The shear viscosity of strongly coupled N = 4 supersymmetric Yang-Mills plasma,” Phys. Rev. Lett. **87**, 081601 (2001) [arXiv:hep-th/0104066]; “From AdS/CFT correspondence to hydrodynamics,” JHEP **0209**, 043 (2002) [arXiv:hep-th/0205052]; P. Kovtun, D. T. Son and A. O. Starinets, “Viscosity in strongly interacting quantum field theories from black hole physics,” Phys. Rev. Lett. **94**, 111601 (2005) [arXiv:hep-th/0405231];

- [12] I. R. Klebanov and M. J. Strassler, “Supergravity and a confining gauge theory: Duality cascades and χ_{SB} -resolution of naked singularities,” *JHEP* **0008**, 052 (2000) [arXiv:hep-th/0007191].
- C. Vafa, “Superstrings and topological strings at large N,” *J. Math. Phys.* **42**, 2798 (2001) [arXiv:hep-th/0008142].
- J. M. Maldacena and C. Nunez, “Towards the large N limit of pure N = 1 super Yang Mills,” *Phys. Rev. Lett.* **86**, 588 (2001) [arXiv:hep-th/0008001].
- I. R. Klebanov and A. A. Tseytlin, “Gravity duals of supersymmetric SU(N) x SU(N+M) gauge theories,” *Nucl. Phys. B* **578**, 123 (2000) [arXiv:hep-th/0002159].
- P. Ouyang, “Holomorphic D7-branes and flavored N = 1 gauge theories,” *Nucl. Phys. B* **699**, 207 (2004) [arXiv:hep-th/0311084].
- I. R. Klebanov and A. A. Tseytlin, “Gravity duals of supersymmetric SU(N) x SU(N+M) gauge theories,” *Nucl. Phys. B* **578**, 123 (2000) [arXiv:hep-th/0002159].
- [13] M. Mia, K. Dasgupta, C. Gale and S. Jeon, “Five Easy Pieces: The Dynamics of Quarks in Strongly Coupled Plasmas,” arXiv:0902.1540 [hep-th]; “The Double Life of Thermal QCD,” arXiv:0902.2216 [hep-th].
- [14] O. Aharony, A. Buchel and A. Yarom, “Holographic renormalization of cascading gauge theories,” *Phys. Rev. D* **72**, 066003 (2005) [arXiv:hep-th/0506002].
- [15] K. Dasgupta, P. Franche, A. Knauf and J. Sully, “D-terms on the resolved conifold,” *JHEP* **0904**, 027 (2009) [arXiv:0802.0202 [hep-th]].
- [16] A. M. Uranga, “Brane Configurations for Branes at Conifolds,” *JHEP* **9901**, 022 (1999) [arXiv:hep-th/9811004].
- K. Dasgupta and S. Mukhi, “Brane Constructions, Conifolds and M-Theory,” *Nucl. Phys. B* **551**, 204 (1999) [arXiv:hep-th/9811139].
- K. Dasgupta and S. Mukhi, “Brane constructions, fractional branes and anti-de Sitter domain walls,” *JHEP* **9907**, 008 (1999) [arXiv:hep-th/9904131].
- [17] P. Ouyang, “Holomorphic D7-branes and flavored N = 1 gauge theories,” *Nucl. Phys. B* **699**, 207 (2004) [arXiv:hep-th/0311084].
- H. Y. Chen, P. Ouyang and G. Shiu, “On Supersymmetric D7-branes in the Warped Deformed Conifold,” *JHEP* **1001**, 028 (2010) [arXiv:0807.2428 [hep-th]].
- [18] M. Becker, K. Dasgupta, A. Knauf and R. Tatar, “Geometric transitions, flops and non-Kaehler manifolds. I,” *Nucl. Phys. B* **702**, 207 (2004) [arXiv:hep-th/0403288]; S. Alexander, K. Becker, M. Becker, K. Dasgupta, A. Knauf and R. Tatar, “In the realm of the geometric transitions,” *Nucl. Phys. B* **704**, 231 (2005) [arXiv:hep-th/0408192]; K. Becker, M. Becker, K. Dasgupta and R. Tatar, “Geometric transitions, non-Kaehler geometries and string vacua,” *Int. J. Mod. Phys. A* **20**, 3442 (2005) [arXiv:hep-th/0411039]; M. Becker, K. Dasgupta, S. H. Katz, A. Knauf and

- R. Tatar, “Geometric transitions, flops and non-Kaehler manifolds. II,” Nucl. Phys. B **738**, 124 (2006) [arXiv:hep-th/0511099]; K. Dasgupta, M. Grisaru, R. Gwyn, S. H. Katz, A. Knauf and R. Tatar, “Gauge - gravity dualities, dipoles and new non-Kaehler manifolds,” Nucl. Phys. B **755**, 21 (2006) [arXiv:hep-th/0605201]; K. Dasgupta, J. Guffin, R. Gwyn and S. H. Katz, “Dipole-deformed bound states and heterotic Kodaira surfaces,” Nucl. Phys. B **769**, 1 (2007) [arXiv:hep-th/0610001].
- [19] G. Bertoldi, F. Bigazzi, A. L. Cotrone and J. D. Edelstein, “Holography and Unquenched Quark-Gluon Plasmas,” Phys. Rev. D **76**, 065007 (2007) [arXiv:hep-th/0702225]; A. L. Cotrone, J. M. Pons and P. Talavera, “Notes on a SQCD-like plasma dual and holographic renormalization,” JHEP **0711**, 034 (2007) [arXiv:0706.2766 [hep-th]]; F. Bigazzi, A. L. Cotrone, C. Nunez and A. Paredes, “Heavy quark potential with dynamical flavors: a first order transition,” Phys. Rev. D **78**, 114012 (2008) [arXiv:0806.1741 [hep-th]]; F. Bigazzi, A. L. Cotrone and A. Paredes, “Klebanov-Witten theory with massive dynamical flavors,” JHEP **0809**, 048 (2008) [arXiv:0807.0298 [hep-th]]; F. Bigazzi, A. L. Cotrone, J. Mas, A. Paredes, A. V. Ramallo and J. Tarrio, “D3-D7 Quark-Gluon Plasmas,” JHEP **0911**, 117 (2009) [arXiv:0909.2865 [hep-th]].
- [20] S. J. Rey, S. Theisen and J. T. Yee, “Wilson-Polyakov loop at finite temperature in large N gauge theory and anti-de Sitter supergravity,” Nucl. Phys. B **527**, 171 (1998) [arXiv:hep-th/9803135]; S. J. Rey and J. T. Yee, “Macroscopic strings as heavy quarks in large N gauge theory and anti-de Sitter supergravity,” Eur. Phys. J. C **22**, 379 (2001) [arXiv:hep-th/9803001]; A. Brandhuber, N. Itzhaki, J. Sonnenschein and S. Yankielowicz, “Wilson loops in the large N limit at finite temperature,” Phys. Lett. B **434**, 36 (1998) [arXiv:hep-th/9803137]; “Wilson loops, confinement, and phase transitions in large N gauge theories from supergravity,” JHEP **9806**, 001 (1998) [arXiv:hep-th/9803263]; D. J. Gross and H. Ooguri, “Aspects of large N gauge theory dynamics as seen by string theory,” Phys. Rev. D **58**, 106002 (1998) [arXiv:hep-th/9805129].
- [21] F. Bigazzi, A. L. Cotrone, A. Paredes and A. Ramallo, “Non chiral dynamical flavors and screening on the conifold,” Fortsch. Phys. **57**, 514 (2009) [arXiv:0810.5220 [hep-th]]; “The Klebanov-Strassler model with massive dynamical flavors,” JHEP **0903**, 153 (2009) [arXiv:0812.3399 [hep-th]].
- [22] S. Kuperstein, “Meson spectroscopy from holomorphic probes on the warped deformed conifold,” JHEP **0503**, 014 (2005) [arXiv:hep-th/0411097].
- [23] R. McNees, R. C. Myers and A. Sinha, “On quark masses in holographic QCD,” JHEP **0811**, 056 (2008) [arXiv:0807.5127 [hep-th]].
C. S. Chu and D. Giataganas, “UV-divergences of Wilson Loops for Gauge/Gravity Duality,” JHEP **0812**, 103 (2008) [arXiv:0810.5729 [hep-th]].
- [24] K. Dasgupta, G. Rajesh and S. Sethi, “M theory, orientifolds and G-flux,” JHEP **9908**, 023 (1999) [arXiv:hep-th/9908088].

- [25] S. B. Giddings, S. Kachru and J. Polchinski, “Hierarchies from fluxes in string compactifications,” *Phys. Rev. D* **66**, 106006 (2002) [arXiv:hep-th/0105097].
- [26] D. Mateos and P. K. Townsend, “Supertubes,” *Phys. Rev. Lett.* **87**, 011602 (2001) [arXiv:hep-th/0103030]; D. Mateos, S. Ng and P. K. Townsend, “Tachyons, supertubes and brane/anti-brane systems,” *JHEP* **0203**, 016 (2002) [arXiv:hep-th/0112054].
D. s. Bak and A. Karch, *Nucl. Phys. B* **626**, 165 (2002) [arXiv:hep-th/0110039];
D. s. Bak and N. Ohta, “Supersymmetric D2 anti-D2 strings,” *Phys. Lett. B* **527**, 131 (2002) [arXiv:hep-th/0112034]; D. s. Bak, N. Ohta and M. M. Sheikh-Jabbari, “Supersymmetric brane anti-brane systems: Matrix model description, stability and decoupling limits,” *JHEP* **0209**, 048 (2002) [arXiv:hep-th/0205265].
K. Dasgupta and M. Shmakova, “On branes and oriented B-fields,” *Nucl. Phys. B* **675**, 205 (2003) [arXiv:hep-th/0306030].
B. Chen and X. Liu, “D1-D3 (or $\bar{D}3$) Systems with Fluxes,” *JHEP* **0808**, 034 (2008) [arXiv:0806.3548 [hep-th]].
- [27] B. R. Greene, A. D. Shapere, C. Vafa and S. T. Yau, “Stringy Cosmic Strings And Noncompact Calabi-Yau Manifolds,” *Nucl. Phys. B* **337**, 1 (1990).
C. Vafa, “Evidence for F-Theory,” *Nucl. Phys. B* **469**, 403 (1996) [arXiv:hep-th/9602022].
- [28] K. Dasgupta and S. Mukhi, “F-theory at constant coupling,” *Phys. Lett. B* **385**, 125 (1996) [arXiv:hep-th/9606044].
K. Dasgupta, D. P. Jatkar and S. Mukhi, “Gravitational couplings and Z(2) orientifolds,” *Nucl. Phys. B* **523**, 465 (1998) [arXiv:hep-th/9707224].
K. Dasgupta and S. Mukhi, “A note on low-dimensional string compactifications,” *Phys. Lett. B* **398**, 285 (1997) [arXiv:hep-th/9612188].
- [29] A. Sen, “F-theory and Orientifolds,” *Nucl. Phys. B* **475**, 562 (1996) [arXiv:hep-th/9605150].
- [30] J. M. Maldacena, “Wilson loops in large N field theories,” *Phys. Rev. Lett.* **80**, 4859 (1998) [arXiv:hep-th/9803002].
- [31] S. Digal, O. Kaczmarek, F. Karsch and H. Satz, “Heavy quark interactions in finite temperature QCD,” *Eur. Phys. J. C* **43**, 71 (2005) [arXiv:hep-ph/0505193]; M. Doring, S. Ejiri, O. Kaczmarek, F. Karsch and E. Laermann, “Heavy quark free energies and screening at finite temperature and density,” *PoS LAT2005*, 193 (2006) [arXiv:hep-lat/0509150]; Y. Aoki, G. Endrodi, Z. Fodor, S. D. Katz and K. K. Szabo, “The order of the quantum chromodynamics transition predicted by the standard model of particle physics,” *Nature* **443**, 675 (2006) [arXiv:hep-lat/0611014]; Y. Aoki, Z. Fodor, S. D. Katz and K. K. Szabo, “The QCD transition temperature: Results with physical masses in the continuum limit,” *Phys. Lett. B* **643**, 46 (2006) [arXiv:hep-lat/0609068]; Y. Aoki, S. Borsanyi, S. Durr, Z. Fodor, S. D. Katz, S. Krieg

- and K. K. Szabo, “The QCD transition temperature: results with physical masses in the continuum limit II,” JHEP **0906**, 088 (2009) [arXiv:0903.4155 [hep-lat]].
- [32] N. Brambilla, A. Pineda, J. Soto and A. Vairo, “Potential NRQCD: An effective theory for heavy quarkonium,” Nucl. Phys. B **566**, 275 (2000) [arXiv:hep-ph/9907240]; “Effective field theories for heavy quarkonium,” Rev. Mod. Phys. **77**, 1423 (2005) [arXiv:hep-ph/0410047]; N. Brambilla *et al.* [Quarkonium Working Group], “Heavy quarkonium physics,” arXiv:hep-ph/0412158; N. Brambilla, J. Ghiglieri, A. Vairo and P. Petreczky, “Static quark-antiquark pairs at finite temperature,” Phys. Rev. D **78**, 014017 (2008) [arXiv:0804.0993 [hep-ph]].
- [33] J. Polchinski and M. J. Strassler, “Hard scattering and gauge / string duality,” Phys. Rev. Lett. **88**, 031601 (2002) [arXiv:hep-th/0109174]; “Deep inelastic scattering and gauge/string duality,” JHEP **0305**, 012 (2003) [arXiv:hep-th/0209211].
- [34] H. Boschi-Filho and N. R. F. Braga, “Gauge/string duality and scalar glueball mass ratios,” JHEP **0305**, 009 (2003) [arXiv:hep-th/0212207]; “QCD/String holographic mapping and glueball mass spectrum,” Eur. Phys. J. C **32**, 529 (2004) [arXiv:hep-th/0209080]; H. Boschi-Filho, N. R. F. Braga and C. N. Ferreira, “Static strings in Randall-Sundrum scenarios and the quark anti-quark potential,” Phys. Rev. D **73**, 106006 (2006) [Erratum-ibid. D **74**, 089903 (2006)] [arXiv:hep-th/0512295]; “Heavy quark potential at finite temperature from gauge/string duality,” Phys. Rev. D **74**, 086001 (2006) [arXiv:hep-th/0607038]; C. A. Ballon Bayona, H. Boschi-Filho, N. R. F. Braga and L. A. Pando Zayas, “On a holographic model for confinement / deconfinement,” Phys. Rev. D **77**, 046002 (2008) [arXiv:0705.1529 [hep-th]]; M. Panero, “Thermodynamics of the QCD plasma and the large-N limit,” Phys. Rev. Lett. **103**, 232001 (2009) [arXiv:0907.3719 [hep-lat]].
- [35] E. Eichten, K. Gottfried, T. Kinoshita, K. D. Lane and T. M. Yan, “The Interplay Of Confinement And Decay In The Spectrum Of Charmonium,” Phys. Rev. Lett. **36**, 500 (1976); “Charmonium: The Model,” Phys. Rev. D **17**, 3090 (1978) [Erratum-ibid. D **21**, 313 (1980)]; “Charmonium: Comparison With Experiment,” Phys. Rev. D **21**, 203 (1980).
- [36] O. Andreev and V. I. Zakharov, “Heavy-quark potentials and AdS/QCD,” Phys. Rev. D **74**, 025023 (2006) [arXiv:hep-ph/0604204]; “The Spatial String Tension, Thermal Phase Transition, and AdS/QCD,” Phys. Lett. B **645**, 437 (2007) [arXiv:hep-ph/0607026]; “On Heavy-Quark Free Energies, Entropies, Polyakov Loop, and AdS/QCD,” JHEP **0704**, 100 (2007) [arXiv:hep-ph/0611304]; “Gluon Condensate, Wilson Loops and Gauge/String Duality,” Phys. Rev. D **76**, 047705 (2007) [arXiv:hep-ph/0703010].
- [37] M. K. Gaillard, D. Martelli, C. Nunez and I. Papadimitrou, “Interpolating geometries and gauge/gravity duality,” To Appear. See also the talk at Strings 2010: <http://mitchell.physics.tamu.edu/Conference/string2010/TitleofTalks.html>

- [38] J. Maldacena and D. Martelli, “The unwarped, resolved, deformed conifold: fivebranes and the baryonic branch of the Klebanov-Strassler theory,” *JHEP* **1001**, 104 (2010) [arXiv:0906.0591 [hep-th]].